TWENTIETH CENTURY GEOMORPHIC CHANGES OF THE LOWER GREEN RIVER IN CANYONLANDS NATIONAL PARK, UTAH: AN INVESTIGATION OF TIMING, MAGNITUDE AND PROCESS

Study Number: CANY-00163

Submitted to:

Canyonlands National Park

Alexander E. Walker[1], John C. Schmidt[1], Paul E. Grams[2]

[1]Department of Watershed Sciences

Utah State University

5210 Old Main Hill, Logan, UT 84322-5210

[2]Southwest Biological Center, Grand Canyon Monitoring and Research Center

U.S. Geological Survey

2255 N Gemini Dr., Flagstaff, AZ 86001

June 10, 2019

Final Report

CONTENTS

LIST OF TABLES

LIST OF FIGURES

ABSTRACT

Since the early 20th century, the Green River, the longest tributary of the Colorado River, has narrowed, decreasing available riparian and aquatic habitat.

Initially, the widespread establishment of non-native tamarisk was considered to be the primary driver of channel narrowing. An alternative hypothesis postulated that changes in hydrology drove narrowing. Reductions in total streamflow and changes to flow regime occurred due to wide-spread water development, decreased snowmelt flood magnitude, and the increased cyclicity of wet and dry years. The two hypotheses agree on channel narrowing, but each influences modern river management differently. A tamarisk-driven model of narrowing implies that modern flow management doesn't substantially affect channel change. Conversely, channel narrowing driven by changes in hydrology implies that present flow management decisions matter and continued adjustments to flow regime may result in future channel change.

To understand the roles of decreasing total annual flow, declining annual peak flood magnitude, and changing vegetation communities on 20th century channel narrowing, we investigated channel narrowing along the lower Green River within Canyonlands National Park (CNP). Previous studies agree that the channel has narrowed, however, the rate, timing and magnitude of documented narrowing are only partially understood.

Multiple lines of evidence were used to reconstruct the history of channel narrowing in the lower Green River. This study focuses on channel narrowing, but additionally investigated possible changes to channel depth, identified process, timing and magnitude of floodplain formation. Floodplain formation was described in the field using stratigraphy, sedimentology, and dendrogeomorphology exposed in a floodplain trench. Channel and floodplain surveys were

conducted to determine possible changes in bed elevation. Additionally, existing aerial imagery, hydrologic data, and sediment transport data were analyzed. These techniques were applied to determine magnitude, timing and processes of channel narrowing at multiple spatial and temporal scales.

The floodplain investigation identified a new period of channel narrowing by vertical accretion after high peak flow years of 1983 and 1984. Narrowing was initiated by vertical accretion in the active channel, deposited by moderate floods exceeded more than 50% of the time. Vertical accretion continued in the early 1990s, converting the active channel into a periodically inundated floodplain surface. Suspended-sediment deposition dominated deposits, resulting in the formation of natural levees and floodplain troughs in both inset floodplains. Rates of deposition were highly variable, ranging from 0.03-0.50 m/yr.

The lower Green River within Canyonlands National Park has narrowed substantially since the late 1800s, resulting in a narrower channel. Changes to flood magnitude, rate and timing since 1900, driven by increased water storage and diversion in the Green River basin and declines in annual precipitation, were responsible for inset floodplain formation. Floodplains of the contemporary lower Green River in CNP began forming in the late 1930s and continued to form and vertically aggrade in the 20th century by inset floodplain formation. During this ~~time~~ period, peak flow and total runoff declined due to climatic changes and water development. Analysis of aerial imagery covering 61 kilometers (km) of the Green River in CNP shows that changes to the floodplain identified in the trench are representative of the entire study area. The establishment of non-native tamarisk *(Tamarix spp.)* did not drive channel narrowing, though dense stands stabilized banks and likely promoted sediment deposition. The lower Green River narrowed 12% from 1940-2014, with the majority of narrowing (10% of all narrowing)

occurring from the 1980s to the present. Inset floodplain formation reflects changes to flood magnitude and timing resulting from water development and decreases in natural runoff.

Findings suggest that long-term management of the riverine corridor within Canyonlands National Park will require a greater focus on upstream flow contributions and how those flows are currently managed. Recovery of endangered endemic native fishes, the Colorado pikeminnow (*Ptychocheilus lucius*), and the razorback sucker (*Xyrauchen texanus)*, plays a primary role in determining current flow allocations. Collaboration with upstream stakeholders and managers is necessary to maximize elements of the flow regime that preserve channel width and limit channel narrowing.

INTRODUCTION

In three days in mid-July 1869, nine men in three boats rowed the 160 km length of the lower Green River between the mouth of the San Rafael River and its confluence with the Colorado River. The group, led by John Wesley Powell, rowed, because "The water is as calm as a lake" (W. C. Bradley journal, July 15, 1869, edited by Darrah, 1947). There were few cottonwood trees (*Populus spp.*) in the "symmetrically curved and grandly arched" canyons that Powell (1895) named Labyrinth and Stillwater. Although cottonwoods were "scrubby" and "very scarce," "there is in some places a small table that affords a footing for a few willows" (J. C. Sumner journal, July 14, 1869, edited by Darrah, 1947). On the inside of bends, Powell (1895) observed a "long peninsula of willow-bordered meadow" and "the talus at the foot of the cliff is usually covered with dwarf oaks." These observations and subsequent photographs taken by E. O. Beaman in early September 1871 during Powell's second expedition (Figure 1), as well as photographs taken in the early 20th century (summarized by Webb et al., 2007) describe a wide active channel with abundant emergent sand bars and lined by "dense willow and greasewood

chaparral" (F. M. Bishop journal, September 11, 1871, edited by C. Kelly, 1947) that comprised "a dense jungle of rose-bushes, willows, and other plants" (Dellenbaugh, 1908). The modern channel of the lower Green River is also lined by woody riparian vegetation that forms dense thickets. Although willow and oak are still present, much of the vegetation is non-native tamarisk (*Tamarix spp*.) and today's channel is narrower. There are fewer emergent sand bars, islands, and secondary channels (Webb and others, 2004; Webb and others, 2007).

Riparian and riverine environments play a critical role in providing habitat for threatened and endangered species in the contemporary Colorado River basin (Keller and others, 2014; Merritt and Cooper, 2000; Merritt and Poff, 2010; Mortenson and Weisberg, 2009; Sankey and others, 2015). The dramatically different environments today are responses to three major disturbances, all of which have occurred within the last 150 years: alteration of the hydrologic and sediment regime by dams and impoundments, climatically driven changes in runoff magnitude, and invasion of nonnative tamarisk onto the floodplain and active channel bars.

Dams, diversions, and irrigation withdrawals fragment the Colorado River watershed, disrupting downstream hydrology, sediment supply, and sediment transport characteristics. Flood discharge declines, with the effects extending hundreds of miles downstream (Graf, 1999). The sediment mass balance of reaches immediately downstream from dams are typically perturbed into sediment deficit, resulting in evacuation of sediment from the bed and sometimes from the banks (Schmidt and Wilcock, 2008; Williams and Wolman, 1984). Segments further downstream may be perturbed into sediment surplus (Andrews, 1986; Schmidt and Wilcock, 2008). Concurrently with the construction of dams throughout the watershed, there have been widespread changes to riparian vegetation communities, the most notable being the spread of invasive tamarisk (*Tamarix spp.*) (Auerbach and others, 2013; Merritt and Cooper, 2000; Sher

and others, 2000; Webb and others, 2007). Today, tamarisk is a dominant component of riparian communities (Friedman et al., 2005).

Assessing the impact of non-native vegetation invasion and basin-wide water impoundment, diversion, and withdrawal is complex, due in part to climatically driven shifts in hydrology during the 20th century. The early 20th century was one of the wettest periods in the last 450 years (Woodhouse and others, 2006) and during the last century, total annual runoff declined independent of direct human disturbances to the flow regime. Indirect human disturbances still affected flow. Precipitation remained relatively constant in the 20th and 21st centuries, but increases in temperature contributed to decreasing streamflow and continued temperature increases are expected to drive expected future declines in streamflow (Udall and Overpeck, 2017).

In the Green River, the longest tributary of the Colorado River, construction of large dams, trans-basin diversions, and within-basin diversions for agriculture and other uses altered the flow regime during the last century. Channel narrowing and other geomorphic responses to these flow-regime changes have been documented on different parts of the Green River and its tributaries (Alexander, 2007; Allred and Schmidt, 1999; Andrews, 1986; Gaeuman and others, 2003; Grams and Schmidt, 2002; Grams and Schmidt, 2005; Lyons and others, 1992; Manners and others, 2014). Additionally, tamarisk spread rapidly through the basin in the early to mid-20th century. On the unregulated Yampa River, colonization by tamarisk, in conjunction with a shift in the natural flow regime, facilitated channel narrowing by trapping sediment and reducing floodplain erosion (Manners and others, 2014).

Comparatively little research has been conducted in the most downstream part of the Green River, where it flows through Canyonlands National Park (CNP) (Birken and Cooper,

2006; Graf, 1978; Webb and others, 2004; Webb and others, 2007). Historic channel narrowing is readily evident in this reach. The wide channel with numerous bare sand bars described by the Powell expedition is now a narrower river with fewer in-channel features. The area of backwater habitat has generally decreased, with likely adverse effects on native fish populations (Bestgen and Hill, 2016).

This study of the lower Green River sought to better understand the magnitude, timing and processes of geomorphic change during the 20th century and in doing so, resolve the differing conclusions of Graf (1978), Andrews (1986), Allred and Schmidt (1999), and Birken and Cooper (2006) regarding the roles of streamflow and invasive vegetation on channel narrowing. To resolve differences, we integrate data collected at the site, cross-section and reach scale on the lower Green River. A multi-scale approach has not been previously applied to investigate channel change in this location and offers the ability to create a unified conceptual model of channel change.

The lower Green River flows through Canyonlands National Park (CNP) and park managers, motivated by goals of ecosystem protection and management for this segment of river, desire a clear understanding of historical geomorphic changes and the mechanisms of such changes. At present, CNP has an incomplete understanding of how invasive vegetation and hydrology influence floodplain formation and channel narrowing. Quantifying rates and timing of narrowing, along with identifying causes of channel narrowing, will provide CNP with detailed information on the geomorphology of the lower Green River that hopefully will improve future park management policies. Understanding whether or not the lower Green River continues to narrow or has established a new equilibrium width is important in managing the riparian corridor, backwater habitat for endangered fishes, sandbars for recreational use, and releases

from upstream reservoirs. Understanding how changes in width influence the formation and maintenance of backwaters is particularly important because the entire lower Green River is designated critical habitat for the endangered razorback sucker (*Xyrauchen texanus*) and Colorado pikeminnow (*Ptychocheilus lucius*) (U.S. Fish and Wildlife Service, 1994).

Channel change and channel width

Changes to flow regime and sediment supply alter the influx and efflux of transported sediment in a river reach, which may drive changes in river channel form that optimize the conveyance of water and sediment such that mass balance is reestablished (Lane, 1955). Changes in the influx of sediment may be caused by changes in the flow regime, watershed sediment supply, or the grain size of the supply. Changes to flow regime and supply rate may be caused by upstream impoundments or diversions or by watershed response to changes in precipitation, land use, or vegetation.

The style of channel change is affected by factors such as the degree of valley confinement and the characteristics of riparian vegetation that can trap transported sediment and give strength to banks (Tal and others, 2004). Channel change may include changes in many attributes, including bed material size and distribution, cross-section size and shape, planform configuration and channel slope. Cross-sectional changes can occur to both size and shape of river channels, affecting both channel width and depth. Channel width is generally adjusted to the magnitude of common floods and when flood magnitude declines, channels narrow (Leopold and Maddock, 1953). Decreasing channel width may occur by a diverse range of morphological adjustments, including a decrease in flow resulting in channel abandonment, channel incision with no new floodplain formation or inset floodplain formation (see Thorne, 1998 for a review of river width adjustments). Additionally, active mid-channel bars can convert to stable, vegetated

islands, reducing active channel width.

Previous research

Previous studies of channel change on rivers with high suspended loads described channel narrowing by deposition of an inset floodplain in the Powder River, Montana (Pizzuto, 1994a), Rio Grande, Texas (Dean and Schmidt, 2011), Colorado River, Colorado (Pitlick and Cress, 2002; VanSteeter and Pitlick, 1998) and Green River, Utah (Allred and Schmidt, 1999; Grams and Schmidt, 2002) due to changing discharge and altered sediment transport regimes. Inset floodplains on these rivers typically form by vertical accretion. Deposition begins on mid-channel or bank-attached bars during periods of relatively low flow, continuing whenever floods carrying high concentrations of fine sediment inundate the aggrading deposit. As sediment is deposited, floodplains vertically accrete, typically forming levees at the channel margin (Dean and others, 2011; Ferguson and Brierley, 1999; Pizzuto and others, 2008). The coarsest suspended sediment is deposited on levees and finer silts and clay deposit in back-basin depressions, or troughs (Dean and others, 2011; Pizzuto and others, 2008). Inset floodplain formation additionally involves colonization of low-elevation bars by vegetation which helps stabilize the bar and promotes sediment deposition (Manners and others, 2014; Shafroth and others, 2002).

In the 20th century, channel narrowing by inset floodplain formation occurred along both the Colorado River and the Green River. Research on the Colorado River, near Grand Junction, Colorado, identified upstream water development (VanSteeter and Pitlick, 1998) and fine sediment deposition by the floods of 1983 and 1984 (Pitlick and Cress, 2002) as causes of inset floodplain formation. In the Green River, upstream from the Yampa River, changes to flow and the resulting channel changes are primarily determined by operations of Flaming Gorge Dam

(Grams and Schmidt, 2002, 2005; Alexander, 2007), whereas the regime of the Green River downstream from the Yampa River is additionally affected by diversions in tributaries. Trans-basin diversions constructed on the Duchesne River reduced streamflow by 50% concurrent with an increase in fine sediment supply causing channel narrowing and bed aggradation (Gaeuman et al., 2005). Construction of dams in the White River basin reduced peak flow by 32% and total flow by 8% from that tributary after the mid-1960s. Flow regulation in the headwaters of the San Rafael River decreased flood magnitude and shifted flood timing, resulting in aggradation within the alluvial valley and simplification of channel planform in a formerly wide channel (Fortney, 2015). Channel narrowing is also observed on unregulated rivers. In the unregulated Yampa River tributary, Manners et al. (Manners and others, 2014) demonstrated narrowing by tamarisk invasion into the active channel during multi-year droughts.

Tamarisk was sparsely distributed along the lower Green River in the 1940s (Clover and Jotter, 1944) and was densely distributed by the 1950s (Christensen, 1962; Graf, 1978). Dense stands of tamarisk are evident in photographs taken in the early 1950s. Today, large areas of tamarisk have been defoliated by the tamarisk beetle (*Diorhabda spp.*) and may be dead, but the skeletal woody stems and roots remain.

The first study of channel change in the lower Green River by Graf (1978) concluded that invading tamarisk had trapped and stabilized fine sediment, inducing channel narrowing on formerly active bars, stabilizing banks, and narrowing the channel. Graf (1978) estimated that the channel narrowed by approximately 27% within CNP between the early 20th century and the 1950s, and he estimated that the channel did not narrow significantly after 1951 despite construction of upstream dams and diversions in the 1960s and 1970s. All subsequent studies agree that the modern channel is narrower than the channel in the early 20th century, and there is

consensus that the invasion of tamarisk on the lower Green River began in the 1930s. Different studies, seeking to clarify some of Graf's (1978) findings, reached different conclusions about when narrowing began, if narrowing eventually stopped or is progressive, and whether tamarisk or changes in flow regime are the primary cause of narrowing. Despite the differing conclusions, Graf's (1978) work remains influential in highlighting the contribution of riparian vegetation invasion to channel narrowing (Birken and Cooper, 2006; Scott and others, 1996).

Everitt (1979) observed that narrowing occurred during a period of declining streamflow, and he suggested that tamarisk may only have played a passive role in channel narrowing. Andrews (1986) analyzed suspended sediment data measured at Green River, Utah. He argued that the effective discharge of the Green River had been reduced after the completion of Flaming Gorge Dam in 1963 allowed reservoir releases to control floods and increase baseflows. He predicted the equilibrium width of the post-dam river using hydraulic geometry relations for the post-dam effective discharge. Because the Green River in the mid-1980s was still wider than than the predicted equilibrium value in 1985, Andrews (1986) predicted further narrowing of the lower Green River.

Allred and Schmidt (1999) compiled and analyzed discharge measurement notes that describe the channel cross-section at current and former U.S. Geological Survey (USGS) gage locations near Green River, Utah. They concluded that channel narrowing had occurred in two phases, one related to a climatically-induced reduction in total streamflow in the mid-20th century and one related to flood control associated with operations of Flaming Gorge Dam. Their findings were applicable to a 26-km study segment, because the temporal pattern of narrowing that had occurred at the Green River, Utah gage had also occurred throughout the Gunnison Valley.

Birkin and Cooper (2006) dated tamarisk and cottonwood trees and excavated pits in order to describe processes of tamarisk invasion and floodplain formation for a 2-km reach of river centered on Potato Bottom at river mile (RM)[1] 37, consistent with the findings of Graf (1978) that the majority of narrowing occurred before 1951 and that channel width remained relatively stable between 1976 and 2002. They argued that tamarisk had played an active role in narrowing, with vegetation establishment triggering bar stabilization, sediment accretion, and the attachment of bars and islands to channel banks.

STUDY AREA

The Green River drains 124,600 square kilometers (km^2), flowing 1,175 km from the Wind River Mountains of Wyoming, through Colorado and Utah, to join the Colorado River in southeastern Utah. Green River, Utah is the former site of Gunnison Crossing in Gunnison Valley, 193 km upstream from the Colorado River confluence. In Gunnison Valley, the Green River has carved a wide alluvial valley into the erodible Cretaceous Mancos shale. The only major tributary downstream of Green River, Utah, the San Rafael River drains the east side of the Wasatch Plateau (drainage area of 6,255 km^2), joining the Green River in Gunnison Valley. A large part of the San Rafael watershed is in the San Rafael Swell and San Rafael Desert where fine sediment yield is high (Fortney, 2015).

Downstream from the San Rafael-Green confluence, the lower Green River carves through progressively older Jurassic to Permian Mesozoic sedimentary rocks, forming canyons. The upstream end of Labyrinth Canyon is approximately 3 km downstream from the San Rafael River where Navajo Sandstone is first exposed at river level. Farther downstream, the cliff-forming Wingate Sandstone and the erodible Moenkopi Formation are exposed. The downstream

[1] Measured upstream from the Colorado River confluence. The location system of River Miles was established by Herron (1917) and is still used today.

end of Labyrinth Canyon is approximately 58 km upstream from the Colorado River confluence, where the White Rim Sandstone emerges, followed by the Organ Rock, Cutler, and Elephant Canyon Formations in Stillwater Canyon. The alluvial valley in Stillwater Canyon is narrower than in Labyrinth Canyon, and there are smaller floodplains and terrace patches. The names of these two canyons were given by John Wesley Powell, who also named the transitional area between the two canyons as Tower Park (Powell, 1895), although this name is infrequently used today.

In this study, we use the term "floodplain" to reference flat lying alluvial landforms adjacent to the river channel and inundated by the current flow regime. This definition encompasses two inset floodplains, at different elevations above the river channel, both containing sediment deposited in the current flow regime, as demonstrated below. We use the term "valley floor" to refer to alluvial landforms above floodplains which are never inundated in the present flow regime.

The banks and bed of the lower Green River are alluvial, and primarily composed of fine sediment (sand, silt and clay). Isolated bedrock banks are present. Gravel is scarce or nonexistent on the channel bed, although Pleistocene gravel terrace deposits occur in Labyrinth Canyon (Pederson and others, 2013).

In this study, we use the term 'lower Green River' to describe a 155-km segment of river beginning at the mouth of the San Rafael River and ending at the Green-Colorado confluence. CNP manages the downstream 76 km of the lower Green River, and the Bureau of Land Management manages the 79 km of river between Green River, Utah and CNP.

The study area is a 61-km portion of lower Labyrinth Canyon and upper Stillwater Canyon, centered in Tower Park. The study area extends from 4 km upstream of Hell Roaring

Canyon at River Mile (RM) 57.5 to 3.8 km downstream of Turks Head at RM 19.5 (Figure 2). The contemporary channel is single-threaded with vertical, vegetated banks, bank-attached active bars, and occasional islands. The floodplain is densely covered by tamarisk and willow (*Salix spp.*). Cottonwoods *(Populus fremontii)* are infrequent, typically mature, and generally located on higher elevation floodplains or the valley floor, above the active channel and floodplain.

The local climate is semi-arid, with 250 millimeters (mm) or less of precipitation annually (Gillies and Ramsey, 2009). The maximum monthly-average precipitation of 31 mm occurs in October and minimum monthly-average precipitation of 10 mm falls in June. The North American (NA) monsoon is active in southern Utah (Adams and Comrie, 1997; Higgins and others, 1997), but its effects are relatively weak. On average, 45% of yearly precipitation falls from July to October (Western Regional Climate Center, 2017). Flash floods are a minimal contributor to total streamflow of the Green River but are a major mechanism for delivering fine sediment to the river (Andrews, 1986).

Streamflow is measured 100 river km upstream from the study area at RM 120 by the USGS at Green River, Utah (gage 09315000, 1885-1899, 1904-present) and within the study area at Mineral Bottom (RM 52, gage 09328920, 2014-present). Streamflow of the San Rafael River is measured near Green River, Utah (gage 09328500, 1909-1918, 1945-present) and near its confluence with the Green River (gage 09328910, 2015-present). Sediment transport data were collected at Green River, Utah between 1941 and 1984 and continuous suspended sediment data using acoustical sensors, calibrated with occasional physical samples, have been collected at Mineral Bottom since 2014 (GCMRC, 2016; Topping and Wright, 2016).

The Green River's annual flow regime is dominated by the spring snowmelt flood. Iorns et al. (1965) demonstrated the key role of Rocky Mountain snowmelt in the flow regime of the

Green River by estimating the average annual flow of gaging stations throughout the watershed for water years 1914-1957, just before construction of large dams in the 1960s. They estimated that approximately 61% of the total annual flow measured at Green River, Utah entered the Green River from the Rocky Mountains upstream from Greendale, Utah or from the Yampa River upstream from Maybell, Colorado. An additional 24% of the total annual flow was delivered to Green River, Utah from the headwaters of the Duchesne and White Rivers. In contrast, less than 2% of the annual flow at Green River, Utah was contributed from the Price River. An additional 2% of flow was added downstream of Green River, Utah by the San Rafael River.

METHODS

Hydrologic analysis

We analyzed the streamflow record at Green River, Utah for changes to peak annual discharge, mean annual discharge and mean daily discharge, all in cubic feet per second (ft^3/s), to determine the timing and scale of 20^{th} century hydrologic changes. We employed a change-point analysis using the nonparametric Pettitt test (Pettitt, 1979) to detect changes in the mean of peak flow distribution (Villarini and others, 2009) at the 5% significance level. A Pettitt analysis checks for shifts in flow regime by identifying abrupt changes in the mean or variance of the variable of interest (in this case, peak flows). The Pettitt test allows for detection of changes when the time of the change point is unknown and is less sensitive to outliers than other change point analyses (Villarini and others, 2009). For each flow period determined by change points, we calculated flood frequency curves, mean annual discharge and mean daily discharge. To describe flood frequency, we characterized high and low peak flow years based on whether peak annual flow was greater than the 75th percentile or less than the 25th percentile, respectively, of

the average for each period of flow regime (Table 1). Periods of 3 or more years above the 75th percentile or below the 25th percentile were classified as clusters of high or low peak flow.

Potential effects of San Rafael River summer and fall flash floods on CNP hydrology are unaccounted for at Green River, Utah, so we additionally analyzed flows in late summer and early fall for the San Rafael River gage. To evaluate the effects of the San Rafael River on the hydrology of the lower Green River, daily discharge was estimated for 1909-1918 and 1945-2015 by adding the mean daily streamflow of the Green River and the San Rafael River. The San Rafael gage did not collect discharge between 1918 and 1945. The two gages measure streamflow from 96% of the watershed area upstream from the Mineral Bottom gage; the ungaged 5,392-km^2 are primarily in the San Rafael Desert, west from the Green River, where precipitation is minimal. Visual inspection of the data show a difference in peak flow timing of one day between the estimated and Mineral Bottom gage records. Therefore, we shifted the estimated flow one day forward so that upstream daily discharges were coincident with Mineral Bottom daily discharge. To evaluate the accuracy of these estimates, we compared the time-shifted estimated daily discharge to the measured mean daily discharge at Mineral Bottom collected since March 2014 (Figure 3). The linear fit between the time-shifted estimated and the observed Mineral Bottom discharge is

$$Mineral\ Bottom = 0.996 \pm 0.005\ Estimated - 17.2\ \pm 32.7 \quad (1)$$

with an R^2 of 0.99. Using the estimated record, we extended the record of streamflow at the Mineral Bottom gage to the period 1909-1918 and 1945-2017, covering 98% of days in those two periods.

The only season when inflow from the San Rafael River can meaningfully affect flow at the Mineral Bottom gage is during summer and early fall when flash floods sometimes occur in

the San Rafael watershed. In order to account for the effect of monsoon floods on floodplain formation, we utilized a peaks-over-threshold analysis (Kidson and Richards, 2005; Lang and others, 1999) to construct a partial duration flood frequency series for peak flows between August 1 and November 1 for all years of the estimated record.

Aerial Imagery Analysis

Ten sets of aerial images taken between 1940 and 2014 were analyzed for changes in width (Table 2). Six series cover the entire study area and two others, 1940 and 1951, cover 90% and 79% of the study area, respectively. The remaining two sets (1976 and 1988) cover a 15-km segment of river (~25% of the study area) centered on Fort Bottom, 64-km upstream from the Colorado River confluence. Six orthorectified image sets (1966, 1993, 2002, 2009, 2011, 2014) are available from public sources. The other sets (1940, 1951, 1976, 1988) were rectified in ERDAS IMAGINE using photogrammetric block calibration. The root mean square error of the rectified images ranged between 0.2 and 1.5 meters (m), depending on scale of the photo set.

Within the study area, bank lines were digitized manually in ArcGIS at a 1:3,000 scale for each year of aerial imagery. The active channel boundary was defined by the presence of vegetation; therefore, the active channel includes the area inundated by water at the time of each photo, as well as emergent bars free of vegetation. The definition of active channel is not dependent on discharge at the time of the photo. Vegetated islands were excluded from the active channel. We did not identify bank lines on the 2011 set because it was taken when the Green River was above flood stage. The 2011 images were used as a comparison set to measure image distortions.

Following digitization of the active channel, we calculated changes in reach-averaged active channel width (m) for each year of available photos (Hughes and others, 2006), in 1-km

reaches by dividing active channel area (square meters, m²) by reach length (m). Total width error, *E* (m), was estimated using a quadratic sum of two independent error estimates (Taylor, 1982): errors associated with bank line digitization and distortion within images:

$$E = \sqrt{p^2 + \theta^2} \quad (2)$$

where *p* is the error associated with digitizing bank lines as a function of the mean width between repeated digitized bank lines (*p*) in meters. For each aerial imagery set, we calculated *p* by repeatedly digitizing bank lines for three 5-km reaches, deriving a centerline from each repeated bank line set in ArcGIS, and taking the mean distance between centerlines as *p* for that set. Image distortion error measurements (θ) in meters were derived by calculating the root-mean-square (RMS) error for each year at 10 floodplain locations that could be identified accurately on all image sets, and comparing those positions to the same locations in the 2011images (Table 3).

Repeat channel surveys

To evaluate whether the documented changes in width were associated with bed incision, bed degradation, or a stable bed, channel cross-sections near Hell Roaring Canyon were reoccupied and the channel bed around Fort Bottom was remapped. Cross-sections near Hell Roaring Canyon were established by the USFWS Upper Colorado River Endangered Fish Recovery Program. Ten cross-sections covering a 3-km reach of the Green River were surveyed on 7 dates in 1995 and 1996 during the spring flood and recession (May-October) by Guensch and Schmidt (1996) to assess changes in Colorado pikeminnow habitat. The reach surveyed is located at a bend in the river, does not contain vegetated islands or side channels, and contains vegetated banks on both sides. Channel surveys around Fort Bottom were first conducted in 1998 by the National Park Service and published in a flow model by Gessler and Moser (2001).

Re-surveys at both sites were performed in 2015 using an Odom CV-100 echo sounder with a 200 kHz transducer inside of the wetted channel combined with an RTK-GPS on the banks. Positioning was by RTK GNSS survey with a local base station set to the coordinate system UTM Zone 12N, North American Datum of 1983 (EPSG 26912). We resurveyed the entire Fort Bottom reach; for cross-sections near Hell Roaring Canyon, 5 complete cross-sections were reoccupied. Single beam sonar data was processed to create a digital elevation model (DEM) of the channel bed. Bathymetric data were merged with Lidar data collected in October 2015 by the state of Utah to produce a combined DEM of the channel and floodplain.

Stratigraphic, sedimentologic, and dendrogeomorphic analysis of floodplain deposits

In August 2015, a 50-m long trench, extending across the entire floodplain, and with a depth of ~2 m, was excavated on the left bank at Hardscrabble Bottom, 2-km upstream from Fort Bottom. The right bank of the river at the trench site is a bedrock canyon wall, and inset floodplain formation is presumed to be confined to the left bank. Stratigraphic units within the trench were mapped and interpreted in the field. Sediment samples were collected from identified units for grain size distributions by a LISST-Portable particle size analyzer (Sequoia Scientific, 2016). Samples from the trench, the Green River and tributaries were collected for clay minerals analysis by X-ray diffraction to determine the bedrock source of these sediments. Ages of deposition for stratigraphic units were determined primarily with dendrochronology using seven tamarisk trees within the trench.

Tamarisk produces distinct annual growth rings and exhibits clear anatomical transformations when buried, making it a viable tree species for dating. For recent sediment deposits of less than 100 years, counting rings is a more accurate floodplain dating method than analysis of ^{14}C, ^{210}Pb and ^{137}Cs isotopes and optically stimulated luminescence (OSL) dating.

Tree-ring methods can date the burial age of a bed to within a year, making it an effective technique to describe processes of floodplain formations across short time scales. Tree-ring analysis is the most comprehensive and accurate method for dating the majority of alluvial deposits in the trench of the available techniques to date floodplains.

We excavated buried tamarisk stems at the margins of the trench, marking each stem with a nail where it intersected a stratigraphic contact, following the procedures established by Dean et al. (2011). After the completion of mapping and interpretation, each tamarisk was removed from the trench for analysis at the USGS dendrochronology lab in Fort Collins, Colorado. Each tree was cut into slabs and each slab was analyzed under a microscope for changes in tree-ring anatomy following the techniques of Friedman et al. (2005b) to determine tree age, germination year and timing of burial events. The age of each deposit was determined at each stratigraphic contact by counting annual rings from the outermost ring inward. Burial was primarily determined by physical changes in tamarisk: narrower annual rings, increasing xylem size in rings, and decreased clarity of annual ring marking (Friedman and others, 2005b). Deposit age was determined from burial year at each stratigraphic contact.

Multiple trees were dated within the same deposits and we cross-dated between multiple trees in the same deposit to increase the accuracy of floodplain deposit ages. Cross-dating compares growth rings of similar widths or physical characteristics between multiple trees. Cross-dating was applied to decrease uncertainty in ring-counting and better constrain ages of deposition. Additionally, cross-dating was applied to date a dead tamarisk in a portionof the trench that did not have any live trees. A dead tree can provide an erroneous age when the tree died prior to being removed from the trench; to accurately date that tree, identical physical characteristics present in both dead and live trees were used as indicator years (Figure 4).

Uncertainty in tree-ring dating was partially constrained for some of the deposits in the trench by determining the possible time period of deposit formation and coupling those time periods with the estimated discharge required to inundate those floodplain deposits. We estimated discharge by calculating a stage-discharge relationship for the Green River at the trench by collecting a range of water surface elevations at the trench and plotting them against daily discharge at Mineral Bottom. A total of 14 measurements were collected at the trench, covering discharges from 74 – 623 m^3/s. The predictive relationship from data collected at the trench is:

$$Q = 1493.2e^{0.6658WSE} \quad (3)$$

where Q is flow (ft^3/s) and WSE is water surface elevation (m). We then compared the trench rating relation to the USGS rating relation for Mineral Bottom, after normalizing the stage elevations for both rating relations to facilitate direct comparisons. The two rating relations are in good agreement, implying the trench rating relation is a good predictor of trench water surface elevations (Figure 5). Inundation levels for each stratigraphic unit combined with the possible period of deposition determined from tree-ring dating together identified a more accurate deposit age. This method decreased uncertainty in age of deposition by an average of 2 years.

For the oldest deposits in the trench, samples were collected and analyzed for date of deposition by the Utah State University Luminescence Lab using the regenerative-dose procedure for single-grain optically stimulated luminesce (OSL) dating. OSL dating determines the last time sediment was exposed to sunlight, and thus, the time since deposition. This technique has large uncertainty if sediment has not been totally reset from its previous burial history or is “partially bleached”. Partial bleaching can happen if sediments are carried in turbid water or transported at night and is a common issue when dating fluvial sediments. The single-

grain approach corrects for these issues by using the minimum age model of Galbraith and Roberts (2012) and can reliably date fluvial deposits (Rittenour, 2008). Two OSL samples were collected in the lowest, farthest onshore end of the trench in what were assumed to be the oldest deposits.

In-channel sedimentologic analysis

The continuous record of suspended sediment transport at Mineral Bottom (GCMRC, 2016), measured by acoustic sensors since March 2014 and calibrated by occasional physical samples, provides a precise understanding of the grain sizes in transport during spring snowmelt, summer, and fall, floods. These are the two flow regimes that potentially contribute to the formation of inset floodplains and channel narrowing, although high suspended sediment concentration flows must attain a stage sufficient to inundate aggrading bars. We analyzed available sediment data to better understand the timing and magnitude of sediment transport. Additionally, we analyzed suspended sediment data and collected bar deposits to determine the different grain size distributions between floodplain, suspended, and in-channel deposits.

RESULTS

Hydrology

Since 1895, there have been three different flood regimes of the lower Green River, based on the Pettitt-test analysis of the peak flow record at Green River, Utah: 1895-1923 (hereafter, "early 20th century"), 1924-1958 (hereafter, "mid-century"), and 1959-2015 (hereafter, "late 20th century") (Table 1). The break point dividing the mid-century and late 20th century flood regimes (1958; $p=<0.001$) is more significant than is the break point dividing the early 20th century from the mid-century flood regimes (1923; $p=0.015$). The 1923 break point occurred at the end of the well-known early 20th century pluvial period of high flows. The second break point, 1958, was

the last large flood prior to closure of Flaming Gorge Dam. These periods are slightly different than the flow regime periods distinguished by Allred and Schmidt (1999) based on visual inspection of the flood record: 1895-1929, 1930-1962 and after 1963. Between 1895 and 1923, the 2-year flood was 41,200 ft^3/s. Between 1924 and 1958, the 2-year flood was 28,500 ft^3/s, and the 2-yr flood was 21,800 ft^3/s from 1958 to 2015 (Figure 7). The largest floods since 1958 occurred in 1983, 1984, and 2011, and the magnitude of these floods was less than the magnitude of the 5-year recurrence flood (54,600 ft^3/s) of the period 1895-1923.

There were no obvious clusters of high flood or low flood years in the early 20th century. After 1923, high peak flows show some evidence of clustering (Figure 7), and the tendency of clustering has remained relatively similar since that time. Clusters of low flood years have only occurred since 1985. High flows between 1927 and 1929 were immediately followed by low peak flows in 1930 and 1931. Large floods between 1983 and 1986 were followed by small floods between 1987 and 1992.

Mean annual flow at Green River, Utah, declined 32%, from 7870 ft^3/s in the early 20th century period to 5370 ft^3/s in the late 20th century (Figure 8). Declines in mean annual flow were less than in peak flow, because flow regulation at Flaming Gorge Dam controls floods and increases base flows. Thus, mean September-February baseflow discharge increased by 16%, from 2500 ft^3/s in early 20th century to 3200 ft^3/s in late 20th century (Figure 9), and the difference between the magnitude of typical annual flood floods and typical base flows is presently less than at any previous time. Presently, the unregulated Yampa River contributes most of the volume of the annual spring snowmelt flood, and contributions from other upstream tributaries have decreased (i.e., Gaeuman et al., 2005).

As described below, suspended fine sediment sometimes is transported in high

concentrations in summer and fall during the season of the North American monsoon, and we investigated whether those high concentration flows might inundate the floodplain and significantly contribute to vertical aggradation. For the period of overlapping measurements at Mineral Bottom and of the San Rafael River, summer and fall floods from the San Rafael contributed only a small part of the total annual flow. For summer and fall months of 2014-2016, the San Rafael River contributed 5% or more of the daily discharge measured at Mineral Bottom on only 7% of all the days.

Although the annual snowmelt flood has frequently overtopped the channel banks and inundated the floodplain, very few summer or fall floods have done so, and no summer or fall flood has inundated a significant part of the floodplain since 1951. We estimated that the lowest trench deposits were inundated at discharges of more than ~7000 ft^3/s, and the current floodplain is inundated at ~ 22,000 ft^3/s. The maximum estimated flow of the lower Green River in the study area during summer and fall for the period 1909-1918 and 1945-2017 exceeded 10,000 ft^3/s in 12% of all years. The estimated flow of the lower Green River has not exceeded 13,000 ft^3/s in summer or fall since 1951. Flow duration curves of the entire flow year measured at Green River, Utah and estimated at Mineral Bottom are not significantly different (Figure 6), further demonstrating that the San Rafael River contributes a relatively small amount of water during most of the year.

Changes to channel size and shape

Mean channel width in the study area measured by aerial imagery analysis decreased by 12% from 138 ± 3.4 m in 1940 to 122 ± 2.1 m in 2014 (Figure 10, Table 3). Width decreased episodically and was relatively stable from 1940 to 1966 but then narrowed 5 m from 1966 to 1993. The 1976 and 1988 imagery, covering a 15--km segment centered on Fort Bottom (RM

44.5-36), more precisely identifies the period of narrowing as having occurred between 1976 and 1988, despite the occurrence of large floods between 1983 and 1986. The rate of channel narrowing increased after 1988. Between 1988 and 1993, channel width near Fort Bottom decreased from 146 ± 2.2 m to 134 ± 4.0 (Figure 10, Table 3). The entire study area narrowed on average 9 m from 1993-2009 to a mean width of 122 ± 2.1 m in 2009.

Narrowing was the net result of inset floodplain formation in some places and bank erosion elsewhere (Figure 11). Our analysis of aerial photographs never indicated a time period when there was no bank erosion, even at times when the channel narrowed significantly. As the channel has narrowed, channel width has become more homogenous since 1993 and is now approximately the same width everywhere (Table 3). The range of channel widths increased slightly in 2014 but was still more homogeneous than prior to 2002. Much of the homogenization of channel width occurred because the formerly wide parts of the channel narrowed more than elsewhere. Maximum observed width decreased by 68 m between 1940 and 2014, but minimum channel width only decreased by 6 m.

The primary process of inset floodplain formation was conversion of bare sand bars to vegetated floodplains (Figure 13). Both bank-attached and mid-channel bars were converted from bare sand to vegetated floodplains since the 1940s. As bars and islands became more densely vegetated, small secondary channels aggraded, decreasing active channel area. The majority of deposition occurred at bars on the inside of bends and adjacent to existing alluvial floodplains. Bedrock banks of the river remained stable and little new floodplain deposition occurred in these places. Sixty percent of all narrowing that occurred in the Fort Bottom segment between 1988 and 1993 was due to the conversion of one large sand bar (118,460 m^2) to floodplain (Figure 14). This conversion narrowed channel width at RM 36.5 by 57 m.

There is no evidence that the channel incised or aggraded during the past 20 years of available survey data, based on comparison of surveys made in 2015 with surveys near Fort Bottom made in 1998 and surveys made near Hell Roaring Canyon in 1995. Although the bed elevations were somewhat higher in one segment and lower in the other, and the measured differences did not exceed the typical magnitude of scour and fill that occurs on the Green River. Thus, the bed elevation differences cannot be distinguished between channel behavior and channel change.

Point density of the 1998 Fort Bottom surveys was too sparse to create an accurate DEM, so we compared the 1998 survey points to our 2015 DEM where the two datasets intersected. Within the 2015 active channel, much of the channel was higher in 2015 than in 1998 (Figure 12), but the two channel surveys were conducted at very different discharges: 22,600 ft^3/s in 1998 and 11,500 ft^3/s in 2015, and bed scour might have been occurring over much of the bed at the time of the 1998 survey.

Near Hell Roaring Canyon, surveys were conducted on 8 different dates at discharges ranging from 3280 to 26,000 ft^3/s in 1995, 1996 and 2015. Three cross-sections were surveyed on all dates (Table 4). Those three cross-sections were merged to create a composite cross-section, that composite cross-section doesn't show any readily identifiable pattern of annual scour during spring snowmelt floods. Mean and maximum channel depth varied by 0.1 m and 1.0 m respectively, between the highest and lowest discharge surveys, and neither depth characteristic is strongly related to discharge. The largest observable change between 1996 and 2015 is an increase of mean depth between July 1, 1996 (10,300 ft^3/s) and May 15, 2015 (10,800 ft^3/s). The average width/depth ratio of the three cross-sections changed from 28.6 in 1996 to 23.2 in 2015 suggesting that the channel bed may be lower today than two decades ago.

However, the 2015 survey was conducted during spring snowmelt and there was no corresponding survey conducted during late summer low flows. Further, changes to channel depth are of a similar magnitude to scour and fill documented in the 1995-1996 surveys (Guensch and Schmidt, 1996). In addition, the measured differences are within the range of annual scour and fill measured upstream at the Green River, Utah gage where Allred and Schmidt (1999) observed scour during snowmelt flooding and fill as discharge receded.

Sedimentology and stratigraphy of floodplain and in-channel deposits

At the trench location on Hardscrabble Bottom, the topography of the valley floor includes two floodplain surfaces that we distinguished as the higher elevation floodplain (F1) and the lower elevation floodplain (F2). A levee and trough are present on both floodplains. F1 is composed of a vertically accreting levee and trough formation, and an intermediate laterally accreting series of beds. A small strip of desert olive (*Forestiera pubescens*) grows at the offshore edge of F1. F2 is a vertically accreting levee and trough. The F1 sequence of deposits vertically truncates the edge of the valley floor, and in turn, is vertically truncated by F2 (Figure 15). The F2 levee is higher above the trough compared to the F1 levee and is located at the edge of F2 at Station[2] (St.) 3.

Below the surface, the trench is composed of 3 major inset deposits, two vertically accreting levee formations, and an intermediate laterally accreting series of beds (Figure 15B). An additional small inset formed at the offshore edge of the trench at St. 0, 1 m above the base of the trench. F1 is capped by a large, laterally continuous vertically accreted unit of sand deposits; F1 is inset into higher terraces. Beds in the terrace are vertically truncated by F1. We interpreted

[2] Station refers to distance along the trench from the end closest to the river. The trench begins at St. 0 and ends in a terrace at St. 50.

those truncations as a former cut bank. Terrace beds are cross-laminated fine sand and muddy fine sand.

Two beds at base of the terrace deposits dated by OSL are 300 ± 150 and 440 ± 250 years old, respectively (Table 1). Terrace deposits are the oldest in the trench, substantially older than F1 or F2, and the trench encompasses all 20th century inset floodplain formation. Based on OSL ages, we infer the edge of the terrace was the river bank in the late 1800s and early 1900s.

Individual beds within the trench are mixed sands and muds that fine upward within distinct flood units. Units with a higher proportion of sand are tan or buff in color, are often lighter in color than mud dominated units and typically contain ripple forms. Small beds of sand occur throughout the trench, primarily at higher elevations compared to mud dominated units. Mud units generally contain highly visible laminae of red mud. Beds with a large portion of silt-and-clay are present throughout the trench, though generally, those deposits dominated at lower elevations and shoreward of levees. Generally, levee deposits are rippled cross-laminated fining upward units with a higher proportion of sand, which fine onshore into a floodplain trough. Trough deposits are primarily composed of horizontally laminated muds with small laterally continuous beds of sand. Beds typically fine upward. Sand and mud beds are present throughout the trench at all elevations, and beds near the surface are extensively bioturbated and weathered.

Four major depositional facies were identified in the trench: (1) floodplain, (2) channel margin, (3) active channel and (4) large flood deposition (Figure 15C). Beds were identified by texture, color and sedimentary structures, if present. Additionally, bed shape and bed orientation were used as an identifier; levee deposits have a convex shape, beds in the trough have a concave shape, and bank-attached bars dip offshore. Boundaries between beds are typically distinct.

Floodplain Facies

The floodplain facies represents deposition and floodplain growth by creation of a natural levee and subsequent vertical accretion of both levee and trough. The characteristics of levees and troughs are very distinct from each other. Levees are constructed of coarse cross-laminated, sand dominated, units fining onshore into a floodplain trough (Figure 16A and B). Individual beds in the levees typically fine upward. The F1 levee is tan sand, rippled cross-laminated forms migrating onshore. Supercritically climbing ripples are present as well (Figure 16B). The F1 levee is capped by the overbank depositional component. In F2, the levee contains tan cross-laminated sand beds that dip onshore and downstream. Sedimentary structures disappear as the levee transitions into the trough.

Trough deposits are primarily fine horizontally laminated silt-and-clay-dominated laterally continuous sediments with small laterally continuous beds of sand (Figure 16C and D). Trough sediments range in color from light gray to tan and distinctive beds of red sediment are present as well (Figure 16C). The F2 trough is a series of laminated beds dominated by silt and clay. Periodic layers of red silt-and-clay are present. The F2 trough is deposited above the active channel facies inset of F1. Where the F2 floodplain is deposited against older F1 sediments, it dips offshore. More silt-and-clay is present in the F1 trough compared to the F2 trough, and layers are thinner (Figure 16C and D).

Levees and troughs have different grain sizes and sedimentary structures and could possibly be classified as different facies. However, since the formation of the levee means a resultant trough will form as well and levees and troughs occur together, they were treated as a single facies.

Channel Margin Facies

This facies is indicative of deposits at the edge of a channel where sediment is regularly deposited and eroded. Texture consists of mixed sand and silt-and-clay, fining upward, bounded by unconformable contacts (Figure 17). Deposits are a series of inset beds, sharply truncated on all sides, generally dipping offshore (Figure 17B). Thin laminae of red silt-and-clay are present in multiple beds. The channel margin component truncates the F1 levee and the F1 floodplain facies and is truncated by F2 deposits. Boundaries are diffuse and consist of multiple small inset beds. The composition of beds varies, from sand to beds of laminated sand and mud (Figure 17C). Sand beds are rippled cross-laminated units, climbing onshore or offshore, and downstream (Figure 17D). Unique sedimentary structures, not seen elsewhere in the trench, were identified in this facies including flame structures near station 18 (Figure 17A) and a 3D bedform at St. 15.

Active Channel Facies

The active channel facies represents vertical deposition and floodplain formation within the active channel at the time of deposition. Beds are vertically accreted against channel margin deposits, 0.20 to 0.60 m thick and composed of mixed sand to fine sand or silt-and-clay (Figure 18A). Beds are horizontal or dip slightly offshore. Contacts are conformable. Sand and silt-and-clay are typically mixed within beds, occasionally, beds are composed of rippled cross-stratified sand. The active channel facies lies under the floodplain facies, forming the base of F2. A low-elevation deposit of cross-laminated sand is present at the base; it is deposited against older channel margin sediments and dips offshore (Figure 18B). We interpreted this bed as a former bank-attached bar deposited inset of F1, which became the core of F2. Above this are massive,

fining upward beds of sand and mud. This is the only lower elevation location in the trench where sand or sand dominated beds are present.

Large Flood Facies

This facies is indicative of floodplain building though vertical accretion during large floods. This facies forms the upper 1-1.5 m of F1 sediments. Beds are primarily horizontally laminated, vertically accreting tan or red sands, brecciated in the upper 0.5-1 m (Figure 18C and D). In F1 above the floodplain trough, deposits are mostly brecciated red sand and silt-and-clay. Brecciated portions contain isolated, small organic horizons near the surface (Figure 18D). At the offshore edge of F1, complete flood cyclothems, or rhythmites, of fine sands fining upward into silt-and-clay, are present. Above the F1 levee are supercritically climbing ripples, migrating onshore and downstream. The offshore edge of the facies is truncated by F2 deposits.

Grain Size

The contemporary lower Green River is a sinuous channel with a meandering thalweg alternating between deep pools and shallow crossovers. Bank-attached and mid-channel bars are located at bends in the river. These “curvature-driven bars” (Parker and Johannesson, 1989) do not migrate downstream because their locations are controlled by stationary bedrock banks. Bars are primarily composed of sand. In low velocity backwaters and channel margins, thick deposits of silt-and-clay are present, transitioning to sand at higher elevations. Thin drapes of mud occur in the troughs of bedforms. Erosion and deposition of emergent bars is constant during summer low flow periods (Figure 19). An unknown proportion of sediment is transported as bedload by downstream-migrating dunes.

The median suspended sand concentration between March 2014 and June 2017 at Mineral Bottom (GCMRC, 2016) was 97 mg/L (Figure 20A) and the median grain size of

suspended sand was very fine sand - 0.11 mm (Figure 20B). Suspended sand concentrations increase with increasing discharge (Figure 21A), and the median grain size of suspended sand decreases as discharges increases (Figure 21B, Figure 21C). Sand concentrations increase during the spring snowmelt flood and again during the summer/fall flash floods.

The median suspended silt-and-clay concentration for the same measurement period was much greater than sand concentration - 310 mg/L (Figure 20C). Silt-and-clay concentrations are highest during the summer and fall months when upstream flash floods occur but are not controlled by the magnitude of Green River discharge. Silt-and-clay concentrations do not increase significantly during the spring snowmelt flood (Figure 21D). The median suspended silt-and-clay concentration of snowmelt-derived flows in May and June was 850, 1100, and 570 mg/L in 2014, 2015, and 2016, respectively. The median suspended silt-and-clay concentration in August and September was 2400, 410, and 570 mg/L in the same 3 years.

Physical bed sediment samples (n=133) collected as part of Mineral Bottom sediment monitoring (GCMRC, 2016) show the median grain size of bed sand is medium sand - 0.30 mm. Ninety percent of collected bed sediment samples have a median sand grain size between 0.18-0.38 mm, coarser than suspended sand samples, which 90% of the time were between 0.09-0.19 mm. Grain sizes from physical samples collected on the surface of bars near Fort Bottom in February 2017 have a median grain size of 0.095 mm – very fine sand (Figure 22).

The majority of sediment samples collected from the trench and measured by the LISST-Portable were silt-dominated; samples were 70% silt on average. The only samples with a proportion of sand greater than 90% are in the terrace where OSL samples were collected. The active channel, channel margin and large flood facies have similar median grain sizes: 0.05 mm, 0.05 mm, and 0.07 mm respectively. In the floodplain component, levee samples have a median

grain size of 0.05 mm. The finest samples are in the floodplain trough and have a median grain size of 0.02 mm. Trough samples are on average 13% clay; all other locations in the trench have clay percentages of 5% or less. The mean sand percentage is 8% in troughs; all other facies and floodplain levees have mean sand proportions of between 22-37%. No gravel is present in the trench. The median grain size collected for each facies is finer than the median grain size of suspended sediment, bed sediment and bar sediment physical samples (Figure 22).

Grain size distributions comparing samples collected from the trench, in-channel bars, suspended sediment samples, and bed sediment samples show that 90% of trench samples are finer than 0.1 mm and approximately 50% of suspended samples are less than 0.1 mm. difference between each set of samples, with little overlap (Figure 22). Suspended sediment and in-channel bar samples have overlapping grain size distributions. Some interaction occurs between the bed, grains in suspension, in channel bars and the floodplain, however, floodplain building material is primarily sourced from finer suspended sediments and little, if not none, sediment in the floodplain is sourced from the bed.

Clay mineral analysis shows that differences in color mirror differences in chemical composition (Table 6). Red clays are primarily illitic, and are locally sourced, correlating with samples collected from Upheaval Wash, 1-km upstream from the trench. Darker, gray beds of clay contain fractions of smectite, and share physical characteristics with samples collected from the Green River and in the Price River. The majority of deposits in the trench appear to be transported from upstream sources, but horizontal laminae of red sediment present in the trench demonstrate that locally sourced material is also a component of inset floodplains.

Timing of floodplain formation

The history of channel narrowing interpreted from aerial photos provides a large-scale

perspective on channel narrowing whose results are spatially robust; these data provide information about channel change beginning in 1939 when the first aerial photographs were taken. These data were supplemented with temporally precise data that comes from interpretation of floodplain stratigraphy exposed in the trench. Because the oldest tree in the trench germinated in 1939, the seqiemce of floodplain formation we describe using dendrogeomorphology extends for the same period as the available aerial photograph data. When supplemented with scattered old ground-level oblique photographs that were first taken near the study area in 1871 and supplemented with other scattered data such as OSL dates of alluvial sediment, a rich history of channel change of the lower Green River emerges.

There have been four major episodes of floodplain formation or accretion: vertical accretion and levee formation from 1939-1952, lateral accretion from 1957-1982, overbank deposition from 1983-2015, and vertical accretion and levee formation from 1985-2015. The first period of floodplain formation occurred following the recession of high flow in the early 1920s. From 1939-1952, at least 18 m of narrowing and 1.1 m of vertical accretion occurred. Deposits accreted 1.5 m at the levee and 1.0 m in the trough. The 1939-1952 deposits are truncated by unconformable contacts. Following this period, small scale vertical accretion of at least 0.30 m occurred from 1953-1982.

Stratigraphic evidence demonstrates that an active bar vertically aggraded between 1952 and 1982. This aggradation was episodic and a portion of these deposits were eroded in 1975 and an unconformity of 8 years exists in the stratigraphy, at the edge of the 1952-1983 deposits until the next record of deposition began in 1983. Erosion in 1975 was confined to the levee at the edge of the 1952-1983 deposits, because a tamarisk tree excavated 11 m further onshore in the floodplain trough (St. 36) of F1 (or F2) ?? showed no evidence of erosion, vertically accreting

1.5 m from 1939 until 1982. We identified this sequence of erosion and deposition by repeated anatomical changes to a buried tamarisk tree (T25-1 in Figure 15C). The tree showed evidence of burial, a release from burial by an erosion event and then a reburial (Figure 23), a sequence similar to burial of an ash tree on the floodplains of the Potomac River, VA described by Sigafoos (1964). The conversion of buried stem wood to unburied root wood is easily identifiable for the slab in 1952, with a conversion back to stem wood visible after 1975. The tree was then buried again in 1983 and new growth after that point was root wood.

Small annual growth rings were documented in 1983 and 1984 (Figure 4) in all trees excavated from F1. The small annual growth rings were preceded and followed by two large rings relative to the 1983-1984 growth rings. This sequence of large, small, large, growth rings is repeated in all four trees recovered from F1. Three of the four trees displayed scar tissue in a single growth ring, presumably due to insect damage. The damaged annual growth ring precedes the 1983 growth rings by 8 years in each of the three trees. Importantly, scar tissue was present in the dead tree, allowing for cross dating. The consistent size of annual growth rings from 1981-1986 and scar tissue in 1975 were used to better constrain the accuracy of tree-ring dating in F1.

Between 1957 and 1982, floodplain unit F1 accreted at least 10 m laterally and 1.3 m vertically. Floodplain accretion occurred by lateral accretion of fining upward mixed sand and silt-and-clay deposits bounded on all sides by distinct unconformable contacts. These deposits exhibit some characteristics of oblique accretion, accreting both laterally and vertically. However, the stratigraphic evidence does not support the definition of oblique accretion introduced by Page et al. (2003) as *"the lateral accumulation of fine-grained floodplain sediment by progradation of a relatively steep convex bank in association with channel migration,"* because beds do not prograde. Instead, lateral growth was due to repeated deposition of

horizontally laminated, vertically truncated, beds. Erosion in 1975 occurred at a higher elevation than these deposits, and it is likely that some lateral accretion occurred prior to erosion in 1975. Erosion documented in 1975 potentially stripped sediment from both floodplain and channel margin facies in F1.

Lateral accretion of the channel margin facies from 1957-1982 narrowed the channel by at least 10 m and accreted the floodplain vertically 1.25 m. The temporal resolution for ages of the active channel deposits is relatively coarse, because only one tree was excavated, and it was rotted at the center under the ground surface. Thus, only the germination year of the tree, 1957, could be determined. The overbank depositional facies above the active channel facies is laterally continuous and sequence with was dated using the other trees in F1. The oldest age of the overbank depositional component in F1 is 1983, providing an upper limit for the ages of active channel deposits.

From 1983-2015, F1 vertically accreted 1 m, above both the 1939-1952 and 1957-1982 deposits. The primary process of accretion was overbank deposition. This deposit contains super critically climbing ripples, indicating rapid deposition, and no significant surface exposure. The only peak annual flows that reached the elevation of the 1983-2015 deposits occurred in 1983, 1984 and 2011. Tree-ring dating shows major burial events in 1983 and 1984. We infer from the hydrologic and dendrogeomorphic evidence that the majority of this vertical accretion occurred in 1983-1984.

Two facies form F2: the active channel facies and the floodplain facies. The floodplain facies vertically accreted above the active channel facies and both facies extend the entire width of the floodplain. Three tamarisk trees were dated, at St. 1, St. 4.5 and St. 7. It was not possible to cross-date between stems, resulting in uncertainty of ± 2 years for deposit ages from tree-ring

dating in the floodplain (Figure 24). Part of this uncertainty is due to position of the trees in F1. Trees in the tough were buried at a later date than trees located at the levee. Constructing a chronological stratigraphic sequence requires interpolating between trees using lateral continuous stratigraphy and resolution can decline when creating a chronology for an entire sequence of deposits. Thus, some portions of the trench were dated more precisely than others and developing dates for the entire cross section required a decrease in temporal resolution and application of additional lines of evidence in addition to data from individual trees. Accounting for uncertainty, beds at the base of F2 are no older than 1985.

From 1985 to 2015, F2 accreted at least 10 m laterally and 2 m vertically, building a new inset floodplain. The upper portion of the floodplain contains beds of cross-stratified sandy material that forms a natural levee. Formation of F2 began as bank-attached bar deposition inset within pre-1985 deposits. From 1985-1986, vertical accretion built 0.5 m of floodplain. In this period, deposits were inundated more than 50% of the time (Figure 25). Basal deposits were deposited as part of the active channel. From 1987-1992, F2 vertically accreted 0.6 m. During this period, all annual peak flows were of less than 20,000 ft^3/s. Peak discharges during this period were deposited sand and mud but did not erode emergent bars and floodplain. Floodplain formation shifted from deposition on a frequently inundated surface to deposition during episodic, moderate peak flows. Between 1993 and 2004, F2 accreted 0.6 m as the rate of vertical accretion slowed. High peak flows returned in the 1990s, but had decreased effects despite their higher discharges and did not cause increased vertical accretion. The floodplain built slowly after 2004, accreting 0.3 m across the levee and trough from 2004-2015. No evidence exists for floodplain stripping between 2005 and 2015 despite a 44,000 ft^3/s flood in 2011, the 3rd highest since 1959 (Figure 25). F2 continues to vertically accrete when floods are greater than the 2-year

flood (21,800 ft^3/s).

DISCUSSION

The primary mechanism of channel narrowing was the formation of vertically accreting, inset floodplains. We demonstrate that this process from 1940-2015 was vertical accretion. Formation began by the accretion of bank-attached bars as part of the active channel. In the trench, accretion of bank-attached bars occurred during periods of relatively low peak flow, preserving the stability of bar deposits throughout the year. Vertical accretion over the span of 1-2 years converted active channel bars to an intermittingly inundated floodplain. Growth of new floodplains decreased active channel width.

Depositional processes observed in the trench range from deposition under regular inundation in the active channel to infrequent inundation and episodic deposition on the floodplain. Key characteristics of active channel deposition are inset beds, dipping offshore, composed of fine sediment. Floodplain facies are distinguished by a smaller median grain size, and distinctive levee and trough sequences. Channel margin facies are primarily identified by sharp truncations of beds in the facies on all sides and the key characteristic of large flood facies are thick beds of horizontally laminated fine sands.

Formation of F1 and F2 occurred by a sequence of vertically and laterally accreting processes which represent different states of floodplain formation by deposition of suspended sediment. Multiple occurrences of the floodplain component show two possible channel margins at the site, one at F1 from 1939-1952 and one in F2 from 1993-2015. The majority of channel narrowing occurred in the earlier stages of floodplain formation under active channel processes. In F2, deposits transition from active channel to levee formation. That transition does not occur in the excavated F1 deposits. It is likely that the transition to floodplain happened below the base

of the trench. Levee deposits are possibly due to a change in the suspended sediment relationship as deposits vertically accreted or increasing hydraulic roughness from rising vegetation density post-1985.

Germination years of tamarisk trees excavated from the trench (1940, 1957, 1985 and 1988) matched to within two years cohorts identified by Birken and Cooper (2006) – 1938, 1958, 1984 and 1986. The similarity in establishment years supports the tree-ring dating and deposition timing discussed in this study. We were unable to directly relate individual sediment deposits between different floodplain investigations due to insufficient detail in previous studies.

We identified a new process of floodplain formation, deposition during large floods, for the lower Green River. High discharges during the rare flow years of 1983 and 1984 deposited sediment uniformly across F1 This process is similar to episodic aggradation of terraces described by Moody and Meade (2008) during a large flood in 1978 on the Powder River, MT. The thickness of large flood deposits is likely influenced by floodplain vegetation, and floodplain stripping may be limited by vegetation (Griffin and others, 2014; Manners and others, 2014; Phillips and Tadayon, 2006). However, flow magnitude may not have reached the threshold for stripping to occur. High flows did not produce floodplain stripping after 1985 and there is no widening associated with recent high flows. Narrowing after 1985 occurred in years of low peak flow.

Processes of channel narrowing by inset floodplain formation were episodic, and the channel changes we documented happened in a small number of years. Channel widths in the study area were stable for most years, even as vertical accretion took place. Similar to studies on the Powder River, Montana (Moody and others, 1999; Moody and Troutman, 2000) and at Green River, Utah (Allred and Schmidt, 1999), frequency of floodplain inundation declined as inset

floodplain deposits vertically accreted over time. Presumably,as vertical accretion of the post-1985 floodplain continues, depositional events will become less frequent in future years, and the rate of vertical accretion will decrease until floodplain deposition solely occurs during rare years of high peak flow.

The relative roles of flow and vegetation in promoting channel narrowing of the lower Green River are complex and difficult to fully unwind. Channel narrowing occurred after both changes in flow regime and establishment of invasive vegetation. Tamarisk is the dominant riparian species, although increases in the extent of sandbar willow account for much of the vegetation growth within in CNP after 1976 (Mortenson and Weisberg, 2009). Recently formed floodplains and low elevation benches are mixed tamarisk-willow communities. Increases in riparian vegetation density and the transition to stands of both tamarisk and willow presumably influenced floodplain deposition by decreasing velocity of overbank flows and increasing hydraulic roughness (Griffin and others, 2014; Manners and others, 2014). How tamarisk influences river form differently than communities of single-stemmed *Salix exigua* is still unknown.

Flow regime changed at the same time as widespread changes to vegetation communities in the lower Green River. Annual maximum discharge and mean annual flow declined. Years of high and low runoff became more clustered, with multiple high flow years followed by several years of low flow. The inset floodplain formation we documented matches expected declines in channel width as a response to decreases in total discharge (Leopold and Maddock, 1953; Thorne, 1998). Further, our findings are consistent with other studies that observed channel narrowing as a response to decreasing discharge (Allred and Schmidt, 1999; Pizzuto, 1994b).

Tamarisk induced channel narrowing elsewhere in the Green River basin (Manners and

others, 2014) and is considered a contributor to channel narrowing at Green River, Utah (Allred and Schmidt, 1999). No direct evidence exists in the lower Green River that channel narrowing in the lower Green River is a response to the establishment of tamarisk. Recent channel narrowing occurred decades after the establishment of tamarisk and changes to width can be linked to hydrology. Nevertheless, increased deposition and floodplain formation in the 20th century was likely due in part to the spread of tamarisk. Recent studies on the interactions between flow, sediment, and vegetation show that, compared to native cottonwood, tamarisk strongly mediates the creation of surface topography in an equilibrium sediment regime, promoting deposition (Diehl and others, 2017; Manners and others, 2015). On the lower Green River, tamarisk establishment and growth on bars in years of low peak flow resulted in dense stands resistant to scour, contributing to stabilization of banks, and greater floodplain deposition.

Inset floodplain formation is not directly linked to changes in peak flow magnitude. Instead, the stabilization of flood deposits and vertical or lateral floodplain formation is a result of yearly magnitude and timing. In-channel deposits were not remobilized during clusters of low peak flow, subsequently, in-channel bars vertically accreted and converted to floodplain. The role of high flows is at least partially independent of flow regime, because the most recent phase of narrowing occurred well after a shift in flow regime in 1959, beginning instead in a cluster of low peak flow years from 1987-1992. Under this model, lateral channel narrowing will likely occur again during a cluster of low or moderate-to-low peak flow years allowing for bar deposition without erosion, stabilization of in-channel deposits, and conversion of channel to floodplain.

New floodplain growth occurred in the second half of the 20th century, with the greatest narrowing taking place after 1985. From 1976-2002, channel narrowing of 13% took place near

Fort Bottom; over the entire study area, the channel narrowed 8% between 1966 and 2002. The identified narrowing in a period of previously presumed stability is due to multiple factors: a large study area, a longer record to track change and the integration of detailed information from the trench with spatially extensive aerial imagery.

The study area covered both stable and active segments of river and the magnitude of change varies by segment; however, for both our study area and Fort Bottom segment, we document consistent and substantial changes to width since the 1940s. We do not know if there were changes to channel width in the early 20th century on the lower Green River, however, prior to the first aerial photo set in 1940, Graf (1978) determined from an analysis of oblique photos that there were no documented changes in width from 1871-1914 and in 1914, the average width of the lower Green River was 266 m. At Green River, Utah, there was little change in width between 1912 and 1928 (Allred and Schmidt, 1999). After 1929, channel width at Green River, Utah declined, narrowing approximately 5 m between 1930 and 1939 (Allred and Schmidt, 1999). Because flow regime is the same for Green River, Utah and the lower Green River, it is possible that the timing of change is similar at both locations and that changes in width began in the late 1920s.

Our description of channel narrowing near Fort Bottom in response to changes in flow regime agrees with the work of Allred and Schmidt (1999) who described a corresponding sequence of narrowing at Green River, Utah. It is possible that the Green River near Green River, Utah has remained stable since the early 1990s. Analysis of channel change near Green River, Utah between 1984 and present could be used to determine if the recent episodes of narrowing identified in this study are widespread or restricted to the lower Green River, downstream of Green River, Utah. Absence of recent episodes of channel narrowing near Green

River, Utah might suggest that channel width in that segment is adjusted to the current flow regime and an equilibrium state is propagating downstream (*sensu* Andrews, 1986). Comparison of the timing of channel narrowing in the Yampa River (Manners and others, 2014; Merritt and Cooper, 2000) and at Green River, Utah will better link changes in channel width for the lower Green River to other locations in the basin, illustrating effects of hydrologic, vegetative and climatic changes on the entire basin.

Anthropogenic and natural changes in hydrology both play important roles in affecting channel form of the lower Green River. Since 1900, climatically driven declines in runoff have been the primary cause of declines in peak flow magnitude. Anthropogenic effects, in particular Flaming Gorge Dam, contribute to changes in flow regime, by decreasing total runoff, decreasing peak flow magnitude, and increasing base flow. Despite the relatively small impact of upstream water development on past channel narrowing, the lower Green River is sensitive to future changes in peak flow magnitude and timing. The low impact of local tributaries and dominance of snowmelt flooding means that changes to peak flow timing and magnitude will influence downstream morphology and will continue to do so in light of future changes, either climatically or anthropogenically driven.

MANAGEMENT IMPLICATIONS

Abundant evidence demonstrates that the lower Green River significantly narrowed in the 20th century. Narrowing occurred as increasing water development decreased peak flow magnitude and raised baseflow magnitude. Changes to flow regime reduced the amount of sediment transported, decreased the area of regularly inundated channel and scours less vegetation than in the early 20th century. These processes all contributed to floodplain formation, resulting in channel narrowing. Climatically driven declines in precipitation and increases in

temperature decreased total annual runoff during the same time period, contributing to narrowing. Channel narrowing occurred in several phases in the 20th century, beginning in the 1930s and continuing in the 21st century. Decreases in channel width happened after a change in flow regime or in a period of low flow following multiple years of peak flow. The primary mechanism of narrowing was vertical accretion, forming floodplains inset within older floodplain deposits. Decreases in width also occurred by the conversion of mid-channel bars to islands and the abandonment of side channels. Establishment of non-native tamarisk in the lower Green River may have promoted floodplain formation by stabilizing banks and inducing greater deposition.

Decreased channel widths in the lower Green River results in channel simplification because the variability of width decreases and multi-threaded channels are reduced to single channels. Channel complexity may be a proxy for fish habitat (Schmidt and Brim Box, 2004), and simplification of the lower Green River may represent a decrease to available fish habitat (Bestgen and Hill, 2016). To restore channel heterogeneity, future management strategies will benefit from a focus on preserving the current snowmelt flood magnitude, coupled with management of both native and non-native riparian vegetation.

In order to limit channel narrowing and potentially restore a more active channel, we describe two possible future management strategies for Canyonlands National Park: a) collaboration and partnership with upstream water managers and fisheries managers on a flow regime beneficial for CNP, and b) active management of native and non-native riparian vegetation.

Collaboration and partnership with upstream water managers, fisheries managers and other invested parties

Currently, flow regime in the middle Green River, downstream of FGD, is managed to benefit endangered fish species, the Colorado pikeminnow (*Ptychocheilus lucius*) and the razorback sucker (*Xyrauchen texanus)*. Maintaining the geomorphic attributes of the channel produced by the natural flood regime and preserving the natural hydrograph is a priority for managers in the middle Green River (Bestgen, 2015; Bestgen and Hill, 2016). These management plans focus on native fishes in the middle Green River and do not extensively consider the lower Green River. Additionally, current flow regime plans do not take into account other aspects of the river corridor, such as the restoration of riparian cottonwoods (Scott and Miller, 2017).

Contemporary channel widths and emergent bars are maintained by the current flow regime, and preserving the current flow magnitude and timing will help to preserve channel width and limit channel narrowing. Increasing the frequency and augmenting the magnitude of peak floods are the future steps most likely to increase channel heterogeneity and widen the channel. In the absence of increasing flows, and predicted future declining annual runoff, preserving as much of the current flow regime as possible and reducing the number of consecutive years of low peak annual flow will be an effective method to limit inset floodplain formation.

Flow regime in the lower Green River is determined by the upstream natural hydrograph of the Yampa River and controlled flow releases from Flaming Gorge Dam (Allred and Schmidt, 1999; Andrews, 1986; Iorns and others, 1965). Those two inputs are the largest contributors to the hydrograph at Mineral Bottom. The annual Yampa River snowmelt flood contributes the

majority of water in the middle and lower Green River during the April-June spring runoff season. Controlled releases from Flaming Gorge Dam (FGD) provide most of the water flowing through the lower Green River during late summer, fall and winter. If more water is diverted or impounded from the Yampa River basin, a greater portion of the flow would come from the upper Green River, increasing dependence on controlled reservoir releases to maintain the current hydrology of the lower Green River. The full powerplant and bypass capacity of FGD is 8,600 ft^3/s, limiting the ability of reservoir releases to fully replace a natural hydrograph. The inability of FGD to replicate the pre-dam hydrograph means that peak flow magnitude is largely dependent upon unregulated flows from the Yampa River basin.

Increased water development in the Yampa River basin has the potential to change the magnitude and timing of streamflow through the lower Green River and CNP. Changes would likely decrease peak flow magnitude, the timing of peak floods and the quantity of water delivered downstream, affecting geomorphic form and process. Currently, there are no plans for large scale dams or trans-basin diversions in the Yampa River basin, but increasing population and greater energy extraction is projected to decrease total runoff in the coming decades (Yampa/White/Green Basin Roundtable, 2015). The importance of Yampa River flows for the maintenance of native fishes is well understood by managers (Bestgen, 2015), creating an opportunity for collaboration.

Our detailed investigation on the timing of channel narrowing and processes of floodplain formation provides an understanding of how the lower Green River responds to change in flood magnitude and consecutive years of high or low flow. Current conditions maintain a channel with numerous active in-channel bars. To preserve the current level of channel form, snowmelt floods with a magnitude greater than 22,000 ft^3/s (the 2-year flood) and duration of a week

should occur at least 1 out of 3 years. A flood of this type will fully inundate in-channel features and partially inundate floodplains. Flood duration of a week is long enough for sediment to be eroded or deposited and in-channel features to be reworked. The current flow regime supports floods with this recurrence interval and does not require any shifts in the hydrologic operations of FGD. Larger floods are dependent upon natural snowmelt in the Yampa River basin and targeting specific discharges, durations, and recurrence intervals is infeasible. Augmenting Yampa River floods with releases from FGD may be possible to maximize flood magnitude in high runoff years, but research focused specifically on environmental flows is needed.

Future conditions of the lower Green River are susceptible to further declines in peak flood magnitude and fewer large floods. Processes of floodplain formation show new floodplains forming in repeated years of low peak flows. A new phase of channel narrowing is probable if multiple years occur with a peak flow less than 15,000 ft^3/s, similar to the post-1985 narrowing described for the lower Green River. Current and future flow regime cannot be controlled within the boundaries of CNP, and will require collaboration with upstream stakeholders.

Maximizing a beneficial flow regime within CNP will require working closely with upstream water and fisheries managers to craft a plan which benefits the largest number of conservation stakeholders. Future work should involve applying this study and others investigating the geomorphologic characteristics of the Green River (Alexander, 2007; Allred and Schmidt, 1999; Grams and Schmidt, 2002; Grams and Schmidt, 2005; Manners and others, 2014) to update previous studies on flow (Bestgen, 2015; Richter and Richter, 2000) with the long term goal of developing an integrated conservation plan for the middle and lower Green River. Fortunately, the objectives of preserving geomorphic form and endangered fish recovery are complementary. Preserving channel heterogeneity enhances aquatic habitat, and maintaining

the current flow regime assists recruitment of endangered fishes while preserving active in-channel bars.

Active management of native and non-native vegetation

The spread of invasive tamarisk may have altered the magnitude of floodplain formation, but did not affect the timing of channel narrowing detailed in this report. Thus, the efficacy of vegetation removal will be dependent upon the magnitude of subsequent snowmelt floods. Despite the widespread defoliation of tamarisk caused by the tamarisk beetle, dead stems are still present and will mediate fluvial landforms and riparian vegetation communities for the foreseeable future. Both invasive and native vegetation should both be cleared from emergent and low-elevation bars to create substrate which can be easily reworked during snowmelt floods, because the lowest portions of the inset floodplains in CNP are covered with willow, rather than tamarisk. For the goal of clearing new substrate, management of both species is the same, because both provide physically trap sediment and stabilize landforms. Clearing dead and live vegetation will create new substrate which can be modified by peak flows, but the rate of channel adjustment after vegetation removal will depend on flow magnitude, timing and duration in the years following removal.

To maximize the effects of vegetation removal, clearing of vegetation should be timed to early spring and/or early fall. Early spring removal will create bare substrate for snowmelt floods to rework. An early fall removal will clear seedlings, preventing new cohorts of vegetation from stabilizing bars. Clearing mature tamarisk will require complete removal of the tree and root system, because merely cutting trees to the ground surface will not increase bank erosion until the stump and root system decompose (Jaeger and Wohl, 2011). Because vegetation removal is labor-intensive and infeasible for the entire lower Green River, clearing will ideally be focused at

locations where the flow of the river will have the greatest effect; for example, at the outside of bends and the location of former in-channel bars.

REFERENCES

Adams, D.K., and Comrie, A.C., 1997, The North American Monsoon: Bulletin of the American Meteorological Society, v. 78, no. 10, p. 2197–2213.

Alexander, J.S., 2007, The timing and magnitude of channel adjustments in the upper Green River below Flaming Gorge Dam in Browns Park and Lodore Canyon, Colorado: An analysis of the pre-and post-dam river using high-resolution dendrogeomorphology and repeat topographic surveys:

Allred, T.M., and Schmidt, J.C., 1999, Channel narrowing by vertical accretion along the Green River near Green River, Utah: Geological Society of America Bulletin, v. 111, no. 12, p. 1757–1772.

Andrews, E.D., 1986, Downstream effects of Flaming Gorge Reservoir on the Green River , Colorado and Utah: Geological Society of America Bulletin, v. 97, no. 8, p. 1012–1023.

Auerbach, D.A., Merritt, D.M., and Shafroth, P.B., 2013, Tamarix, Hydrology, and Fluvial Geomorphology, *in* Sher, A.A. and Quigley, M.F. eds., Tamarix: a case study of ecological change in the American West: Oxford University Press, p. 99–122.

Bestgen, K., 2015, Aspects of the Yampa River Flow Regime Essential for Maintenance of Native Fishes:

Bestgen, K., and Hill, A.A., 2016, Reproduction, abundance, and recruitment dynamics of young Colorado pikeminnow in the Green and Yampa rivers, Utah and Colorado, 1979-2012. Final report to the Upper Colorado River Endangered Fish Recovery Program, Project FW BW-Synth, Denver, CO.:

Birken, A.S., and Cooper, D.J., 2006, Processes of Tamarix invasion and floodplain development along the lower Green River, Utah: Ecological Applications, v. 16, no. 3, p. 1103–1120.

Darrah, W.C., 1947, Biographical sketches and original documents of the first Powell Expedition of 1869.: Utah Historical Quarterly, v. 15, p. 9–148.

Dean, D.J., and Schmidt, J.C., 2011, The role of feedback mechanisms in historic channel changes of the lower Rio Grande in the Big Bend region: Geomorphology, v. 126, no. 3–4, p. 333–349.

Dean, D.J., Scott, M.L., Shafroth, P.B., and Schmidt, J.C., 2011, Stratigraphic, sedimentologic, and dendrogeomorphic analyses of rapid floodplain formation along the Rio Grande in Big Bend National Park, Texas: Bulletin of the Geological Society of America, v. 123, no. 9–10, p. 1908–1925.

Dellenbaugh, F.S., 1908, A Canyon Voyage: The University of Arizona Press, Tucson, AZ, 267 p.

Diehl, R.M., Wilcox, A.C., Stella, J.C., Kui, L., Sklar, L.S., and Lightbody, A., 2017, Fluvial sediment supply and pioneer woody seedlings as a control on bar-surface topography: Earth Surface Processes and Landforms, v. 42, no. 5, p. 724–734.

Everitt, B.L., 1979, Fluvial adjustments to the spread of tamarisk in the Colorado Plateau region: Reply: Geological Society of America Bulletin, v. 90, no. 12, p. 1184.

Ferguson, R.J., and Brierley, G.J., 1999, Levee morphology and sedimentology along the lower

Tuross River, south-eastern Australia: Sedimentology, v. 46, no. 4, p. 627–648.
Fortney, S.T., 2015, A Century of Geomorphic Change of the San Rafael River and Implications for River Rehabilitation: All Graduate Theses and Dissertations, v. 2.
Friedman, J.M., Auble, G.T., Shafroth, P.B., Scott, M.L., Merigliano, M.F., Freehling, M.D., and Griffin, E.R., 2005a, Dominance of non-native riparian trees in western USA: Biological Invasions, v. 7, no. 4, p. 747–751.
Friedman, J.M., Vincent, K.R., and Shafroth, P.B., 2005b, Dating floodplain sediments using tree-ring response to burial: Earth Surface Processes and Landforms, v. 30, no. 9, p. 1077–1091.
Gaeuman, D. a., Schmidt, J.C., and Wilcock, P.R., 2003, Evaluation of in-channel gravel storage with morphology-based gravel budgets developed from planimetric data: Journal of Geophysical Research, v. 108, no. F1, p. 1–16.
Gaeuman, D.A., Schmidt, J.C., and Wilcock, P.R., 2005, Complex channel responses to changes in stream flow and sediment supply on the lower Duchesne River, Utah: Geomorphology, v. 64, no. 3–4, p. 185–206.
Galbraith, R.F., and Roberts, R.G., 2012, Statistical aspects of equivalent dose and error calculation and display in OSL dating: An overview and some recommendations: Quaternary Geochronology, v. 11, p. 1–27.
GCMRC, 2016, Green River at Mineral Bottom nr Cynlnds Ntl Park 09328920, accessed January 1, 2017, at https://www.gcmrc.gov/discharge_qw_sediment/station/CL/09328920.
Gessler, D., and Moser, E., 2001, Two Dimensional Computer Modeling of Green River at Dinosaur National Monument and Canyonlands National Park:
Gillies, R.R., and Ramsey, R.D., 2009, Climate of Utah, *in* Banner, R.E., Baldwin, B.D., and McGinty, E.I.L. eds., Rangeland Resources of Utah: Utah State University Cooperative Extension, Logan, UT, USA, p. 39–45.
Graf, W.L., 1978, Fluvial adjustments to the spread of tamarisk in the Colorado Plateau region: Geological Society of America Bulletin, v. 89, no. 10, p. 1491–1501.
Graf, W.L., 1999, Dam nation: A geographic census of american dams and their large-scale hydrologic impacts: Water Resources Research, v. 35, no. 4, p. 1305–1311.
Grams, P.E., and Schmidt, J., 2002, Streamflow regulation and multi-level flood plain formation: channel narrowing on the aggrading Green River in the eastern Uinta Mountains, Colorado and Utah: Geomorphology, v. 44, p. 337–360.
Grams, P.E., and Schmidt, J.C., 2005, Equilibrium or indeterminate? Where sediment budgets fail: Sediment mass balance and adjustment of channel form, Green River downstream from Flaming Gorge Dam, Utah and Colorado: Geomorphology, v. 71, p. 156–181.
Griffin, E.R., Perignon, M.C., Friedman, J.M., and Tucker, G.E., 2014, Effects of woody vegetation on overbank sand transport during a large flood, Rio Puerco, New Mexico: Geomorphology, v. 207, p. 30–50.
Guensch, G., and Schmidt, J.C., 1996, Channel Response to High Discharge in 1996, Green River at Ouray and Mineral Bottom:
Higgins, R.W., Yao, Y., and Wang, X.L., 1997, Influence of the North American monsoon system on the U.S. summer precipitation regime: Journal of Climate, v. 10, no. 10, p. 2600–2622.
Hughes, M.L., McDowell, P.F., and Marcus, W.A., 2006, Accuracy assessment of georectified aerial photographs: Implications for measuring lateral channel movement in a GIS:

Geomorphology, v. 74, no. 1–4, p. 1–16.
Iorns, W. V, Hembree, C.H., and Oakland, G.L., 1965, Water Resources of the Upper Colorado River Basin - Technical Report: US Geological Survey Professional Paper 441.
Jaeger, K.L., and Wohl, E., 2011, Channel response in a semiarid stream to removal of tamarisk and Russian olive: Water Resources Research, v. 47, no. September 2010.
Keller, D.L., Laub, B.G., Birdsey, P., and Dean, D.J., 2014, Effects of flooding and tamarisk removal on habitat for sensitive fish species in the San Rafael River, Utah: implications for fish habitat enhancement and future restoration efforts.: Environmental management, v. 54, no. 3, p. 465–78.
Kidson, R., and Richards, K.S., 2005, Flood frequency analysis: assumptions and alternatives: Progress in Physical Geography, v. 29, no. 3, p. 392–410.
Lane, E.W., 1955, The importance of fluvial morphology in hydraulic engineering: Proceedings of the American Society of Civil Engineers, v. 81, p. 1–17.
Lang, M., Ouarda, T.B.M.J., and Bobée, B., 1999, Towards operational guidelines for over-threshold modeling: Journal of Hydrology, v. 225, no. 3–4, p. 103–117.
Leopold, L.B., and Maddock, T.M., 1953, The Hydraulic Geometry of Stream Channels and Some Physiographic Implications: USGS Professional Paper, v. 252.
Lyons, J.K., Pucherelli, M.J., and Clark, R.C., 1992, Sediment transport and channel characteristics of a sand-bed portion of the green river below flaming gorge dam, Utah, USA: Regulated Rivers: Research & Management, v. 7, no. 3, p. 219–232.
Manners, R.B., Schmidt, J.C., and Scott, M.L., 2014, Mechanisms of vegetation-induced channel narrowing of an unregulated canyon river: Results from a natural field-scale experiment: Geomorphology, v. 211, p. 100–115.
Manners, R.B., Wilcox, A.C., Kui, L., Lightbody, A.F., Stella, J.C., and Sklar, L.S., 2015, When do plants modify fluvial processes? Plant-hydraulic interactions under variable flow and sediment supply rates: Journal of Geophysical Research: Earth Surface, v. 120, no. 2, p. 325–345.
Merritt, D.M., and Cooper, D.J., 2000, Riparian vegetation and channel change in response to river regulation: A comparative study of regulated and unregulated streams in the Green River Basin, USA: Regulated Rivers-Research & Management, v. 564, no. January, p. 543–564.
Merritt, D.M., and Poff, N.L., 2010, Shifting dominance of riparian Populus and Tamarix along gradients of flow alteration in western North American rivers: Ecological Applications, v. 20, no. 1, p. 135–152.
Moody, J.A., and Meade, R.H., 2008, Terrace aggradation during the 1978 flood on Powder River, Montana, USA: Geomorphology, v. 99, no. 1–4, p. 387–403.
Moody, J.A., Pizzuto, J.E., and Meade, R.H., 1999, Ontogeny of a flood plain: GSA Bulletin, v. 111, no. 2, p. 291–303.
Moody, J. a, and Troutman, B.M., 2000, Quantitative model of the growth of floodplains by vertical accretion: Earth Surface Processes and Landforms, v. 25, no. 2, p. 115–133.
Mortenson, S.G., and Weisberg, P.J., 2009, Plant community response to Tamarisk invasion and hydrologic regime in the Cataract Canyon, Canyonlands National Park: A preliminary investigation:
Page, K.J., Nanson, G.C., and Frazier, P.S., 2003, Floodplain formation and sediment stratigraphy resulting from oblique accretion on the Murrumbidgee River, Australia: Journal

of Sedimentary Research, v. 73, no. 1, p. 5–14.
Parker, G.P., and Johannesson, H., 1989, Observations on several recent theories of resonance and overdeepening in meandering channels, *in* Ikeda, S. and Parker, G. eds., River Meandering:, p. 379–415.
Pederson, J., Burnside, N., Shipton, Z., and Rittenour, T., 2013, Rapid river incision across an inactive fault--Implications for patterns of erosion and deformation in the central Colorado Plateau: Lithosphere, v. 5, no. 5, p. 513–520.
Pettitt, A.N., 1979, A Non-Parametric Approach to the Change-Point Problem: Applied Statistics, v. 28, no. 2, p. 126.
Phillips, J. V, and Tadayon, S., 2006, Selection of Manning's Roughness Coefficient for Natural and Constructed Vegetated and Non-Vegetated Channels, and Vegetation Maintenance Plan Guidelines for Vegetated Channels in Central Arizona: U.S. Geological Survey, Scientific Investigations Report 2006-5108.
Pitlick, J., and Cress, R., 2002, Downstream changes in the channel geometry of a large gravel bed river: Water Resources Research, v. 38, no. 10, p. 1–11.
Pizzuto, J., 1994a, Channel adjustments to changing discharges, Powder River, Montana: Geological Society of America Bulletin, no. November, p. 1494–1501.
Pizzuto, J.E., 1994b, Channel adjustments to changing discharges, Powder River, Montana: Geological Society of America Bulletin, v. 106, no. November, p. 1494–1501.
Pizzuto, J.E., Moody, J. a., and Meade, R.H., 2008, Anatomy and dynamics of a floodplain, Powder River, Montana, U.S.A.: Journal of Sedimentary Research, v. 78, no. 1, p. 16–28.
Powell, J.W., 1895, The Exploration of the Colorado River and its Canyons: Dover, New York, NY, 397 p.
Richter, B.D., and Richter, H.E., 2000, Prediscribing flood regimes to sustain ecosystems along meandring rivers: Conservation Biology, v. 14, no. 5, p. 1467–1478.
Rittenour, T.M., 2008, Luminescence dating of fluvial deposits: applications to geomorphic, palaeoseismic and archaeological research: Boreas, v. 37, no. 4, p. 613–635.
Sankey, J.B., Ralston, B.E., Grams, P.E., Schmidt, J.C., and Cagney, L.E., 2015, Riparian vegetation, Colorado River, and climate: Five decades of spatiotemporal dynamics in the Grand Canyon with river regulation: Journal of Geophysical Research: Biogeosciences, v. 120, no. 8, p. 1532–1547.
Schmidt, J.C., and Brim Box, J., 2004, Application of a Dynamic Model to Assess Controls on Age-0 Colorado Pikeminnow Distribution in the Middle Green River, Colorado and Utah: Annals of the Association of American Geographers, v. 94, no. 3, p. 458–476.
Schmidt, J.C., and Wilcock, P.R., 2008, Metrics for assessing the downstream effects of dams: Water Resources Research, v. 44, no. April 2006, p. 1–19.
Scott, M.L., Friedman, J.M., and Auble, G.T., 1996, Fluvial process and the establishment of bottomland trees: Geomorphology, v. 14, no. 4, p. 327–339.
Scott, M.L., and Miller, M.E., 2017, Long-term cottonwood establishment along the Green River, Utah, USA: Ecohydrology, no. December 2016, p. e1818.
Sequoia Scientific, 2016, LISST-Portable|XR Manual Version 1.2, at http://www.sequoiasci.com/wp-content/uploads/2015/06/LISST-PortableXRManualVersion1.2-April2016.pdf.
Shafroth, P.B., Stromberg, J.C., and Patten, D., 2002, Riparian vegetation response to altered disturbance and stress regimes: Ecological Applications, v. 12, no. 1, p. 107–123.

Sher, A.A., Marshall, D.L., and Gilbert, S.A., 2000, Competition between native Populus deltoides and invasive Tamarix ramosissima and the implications for reestablishing flooding disturbance: Conservation Biology, v. 14, no. 6, p. 1744–1754.
Sigafoos, R.S., 1964, Botanical evidence of floods and flood-plain deposition: US Geological Survey Professional Paper 485-A.
Stephens, H.G., and Shoemaker, E.M., 1987, In the Footsteps of John Wesley Powell: The Powell Society, Denver, CO, 286 p.
Tal, M., Gran, K., Murray, A.B., Paola, C., and Hicks, D.M., 2004, Riparian vegetation as a primary control on channel characteristics in multi-thread rivers, *in* Riparian Vegetation and Fluvial Geomorphology:, p. 43–58.
Taylor, J.R., 1982, An Introdution to Error Analysis: University Science Books, Sausalito, CA, 349 p.
Thorne, C.R., 1998, River Width Adjustment. I: Processes and Mechanisms: Journal of Hydraulic Engineering, v. 124, no. 9, p. 881–902.
Topping, D.J., and Wright, S.A., 2016, Long-term continuous acoustical suspended-sediment measurements in rivers - Theory, application, bias, and error:, accessed at Professional Paper at http://pubs.er.usgs.gov/publication/pp1823.
U.S. Fish and Wildlife Service, 1994, Determination of Critical Habitat for the Colorado River Endangered Fishes: Razorback Sucker, Colorado Squawfish, Humpback Chub, and Bonytail Chub: Federal Register, v. 59, no. 54, p. 13374–13400.
Udall, B., and Overpeck, J., 2017, The twenty-first century Colorado River hot drought and implications for the future: Water Resources Research.
VanSteeter, M.M., and Pitlick, J., 1998, Geomorphology and endangered fish habitats of the upper Colorado River: 1. Historic changes in streamflow, sediment load, and channel morphology: Water Resources Research, v. 34, no. 2, p. 287.
Villarini, G., Serinaldi, F., Smith, J. a., and Krajewski, W.F., 2009, On the stationarity of annual flood peaks in the continental United States during the 20th century: Water Resources Research, v. 45, no. 8, p. 1–17.
Webb, R.H., Belnap, J., and Weisheit, J., 2004, Cataract Canyon: A Human and Environmental History of the Rivers in Canyonlands: The University of Utah Press, Salt Lake City, UT, 268 p.
Webb, R.H., Leake, S.A., and Turner, R.M., 2007, The Ribbon of Green: Change in Riparian Vegetation in the Southwestern United States: University of Arizona Press, Tucson, AZ, 462 p.
Western Regional Climate Center, 2017, Canyonlands the Neck, Utah (421163), accessed March 12, 2017, at http://www.wrcc.dri.edu/cgi-bin/cliMAIN.pl?ut1163.
Williams, G.P., and Wolman, M.G.G., 1984, Downstream effects of dams on alluvial rivers: US Geological Survey Professional Paper 1286, v. 277.
Woodhouse, C.A., Gray, S.T., and Meko, D.M., 2006, Updated streamflow reconstructions for the Upper Colorado River Basin: Water Resources Research, v. 42, no. 5, p. 1–16.
Yampa/White/Green Basin Roundtable, 2015, Yampa/White/Green Basin Implementation Plan:, accessed April 4, 2016, at https://www.colorado.gov/pacific/sites/default/files/Yampa-WhiteBIP_Full.pdf.

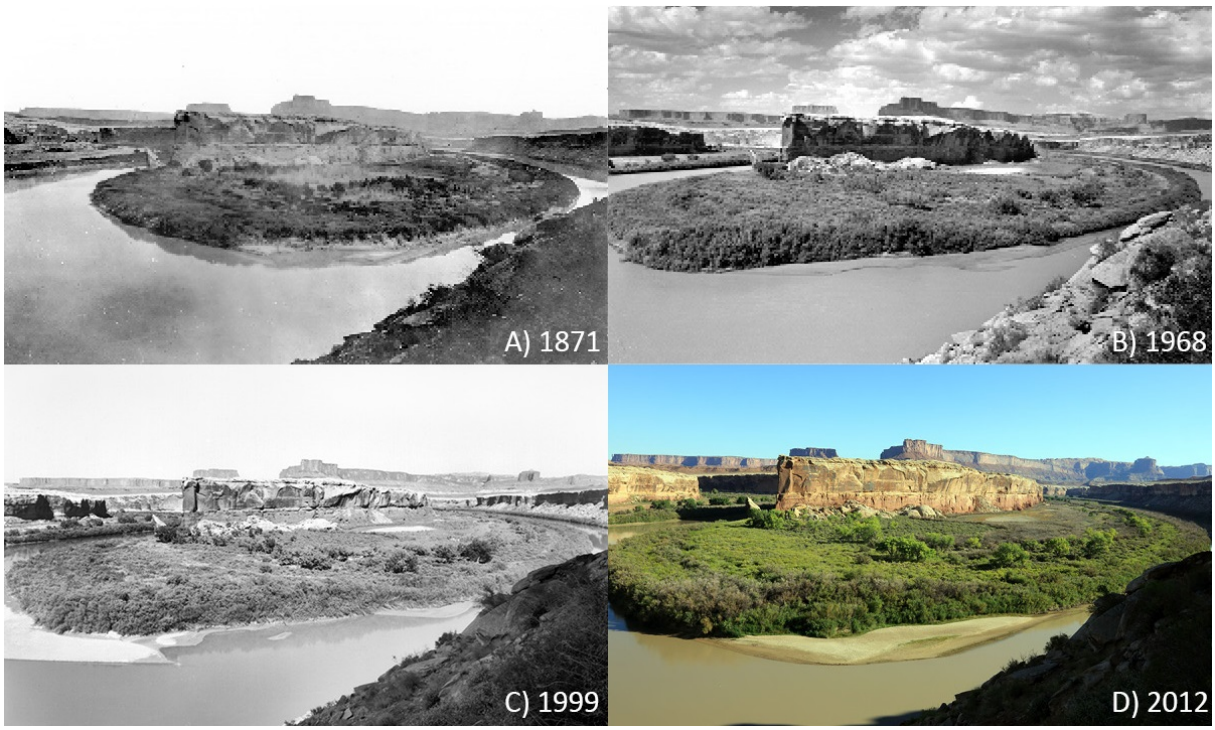

Figure 1: A photo match taken at Bonita Bend, on the lower Green River at RM 30, 50-km upstream from the Green-Grand confluence on the right bank at the apex of the bend, looking east. Flow is from left to right. A) Taken by E.O. Beaman on September 9, 1871 during the second John Wesley Powell expedition. B) Taken by E.G Stephens on August 19, 1968 (Stephens and Shoemaker, 1987). C) Taken by Dominic Oldershaw October 13, 1999 D) Taken by Mark E. Miller September 28, 2012. The channel is wide in 1871 and the banks of the bend are vegetated. In 1968, the channel has narrowed; the vegetation next to the water's edge is tamarisk. Channel width remains stable in the 1999 and 2012 photos. A small emergent bar visible in the center of the 1968 is present in 2012. Tamarisk in 2012 shows widespread mortality due to effects of the tamarisk beetle. Dead tamarisk is purplish-brown in the 2012 photo. Photos courtesy of Southwest Biological Science Center, USGS, Flagstaff, Arizona.

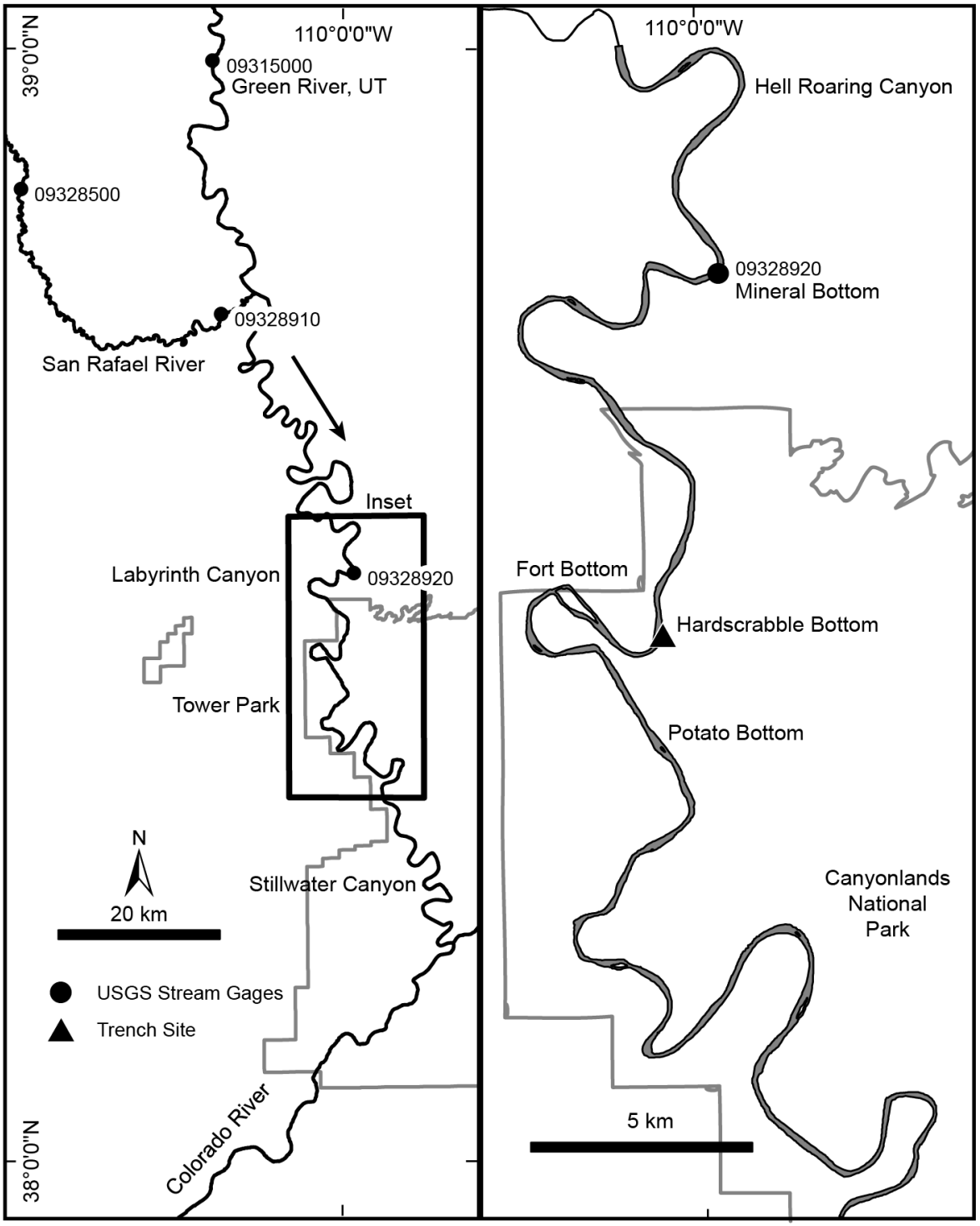

Figure 2: Map of the lower Green River and study area. Gages are 09315000 Green River at Green River, UT, 09328500 San Rafael River near Green River, UT, 09328910 San Rafael River at mouth near Green River, UT and 09328920 Green River at Mineral Bottom, UT. Channels surveys were conducted near Hell Roaring Canyon and Fort Bottom.

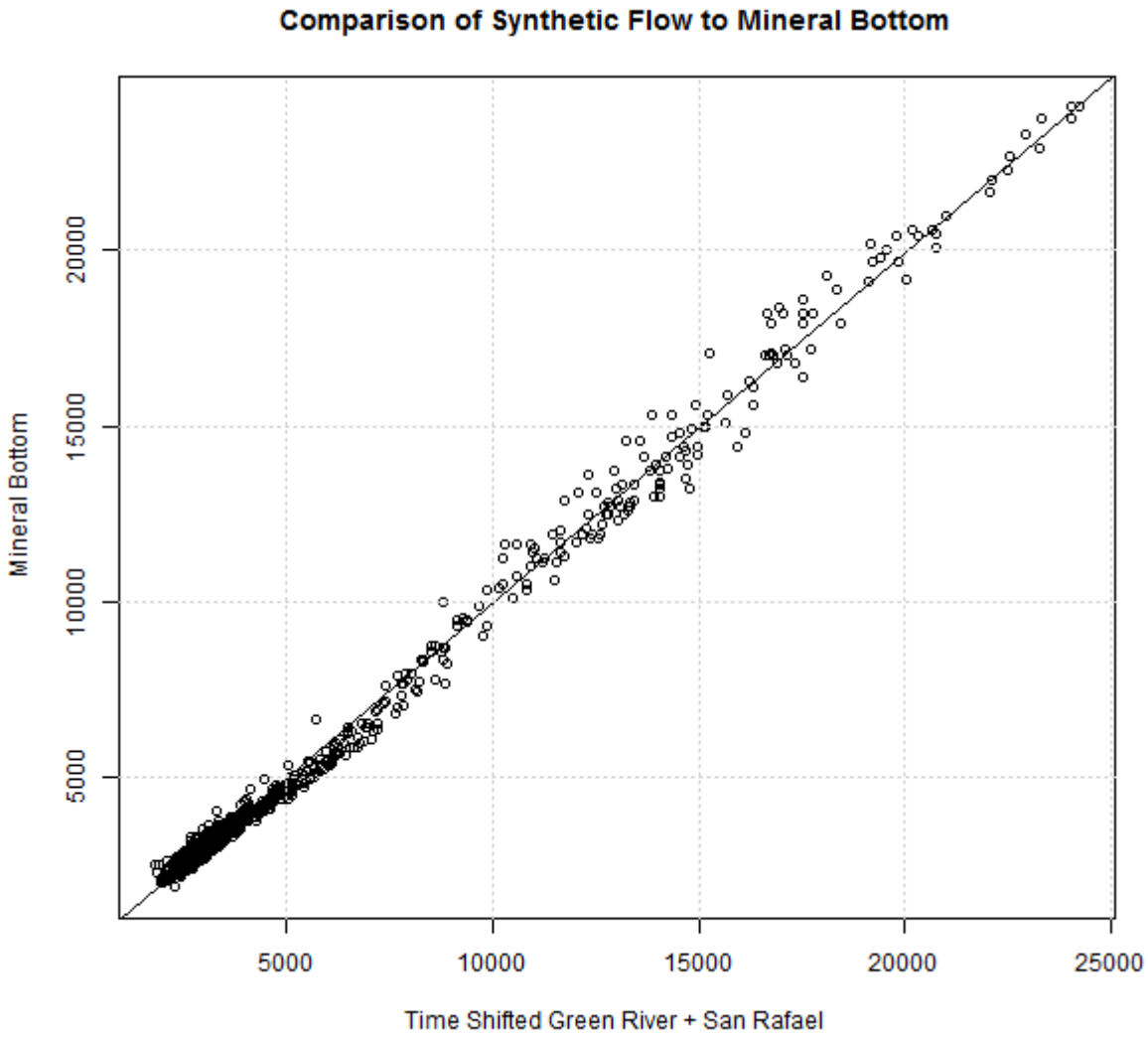

Figure 3: Comparison of daily discharge values for the time shifted estimated flow method (Green River + San Rafael) and data collected at Mineral Bottom, UT from March 3, 2014 to February 1, 2017 (n=1006).

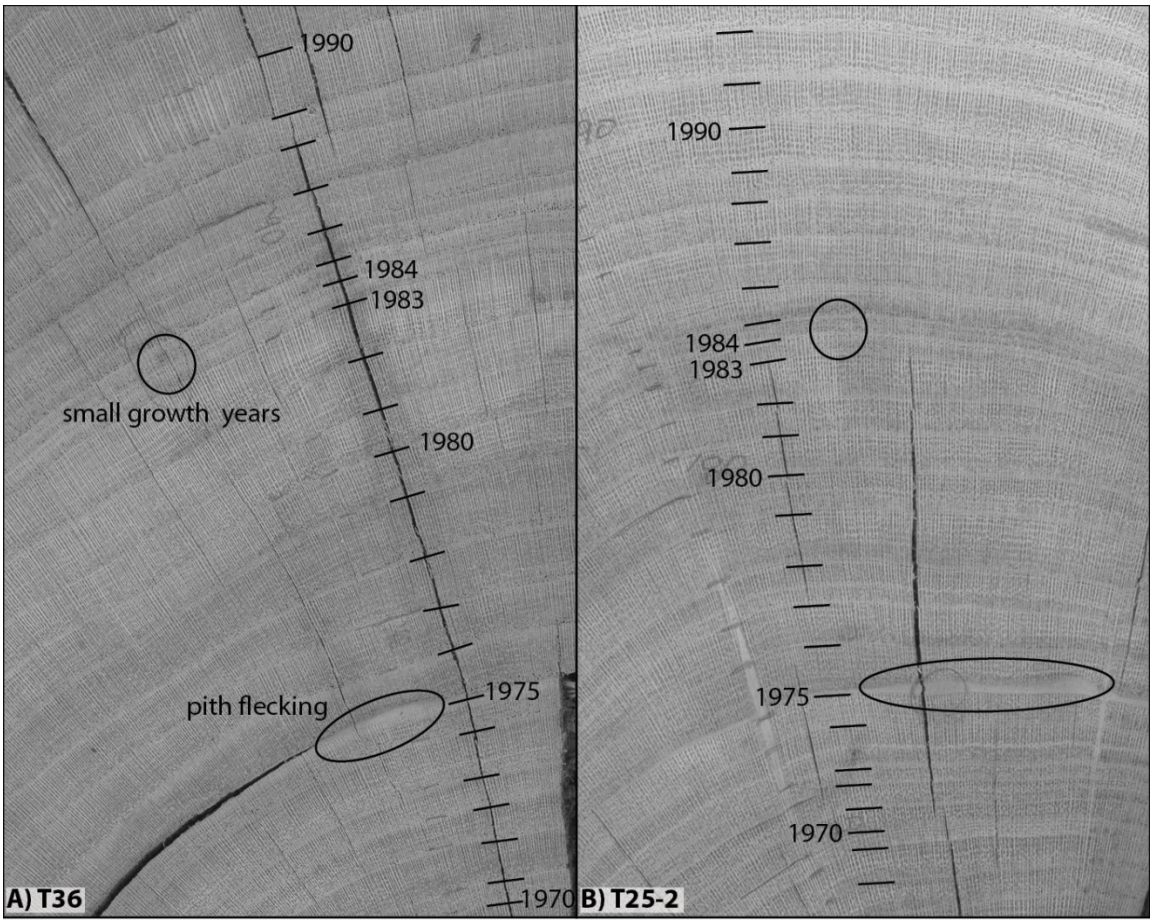

Figure 4: Example of cross-dating between trees. A) is a slab from T36, a live tree, and B), a slab from a dead tree, T25-2. Marks represent annual growth years. The sequence of pith flecking and small annual growth years is the same for A) and B), and the number of rings (years), between the two unique features is identical. Observed physical changes between trees improve tree-ring dating and decrease uncertainty in floodplain deposit ages.

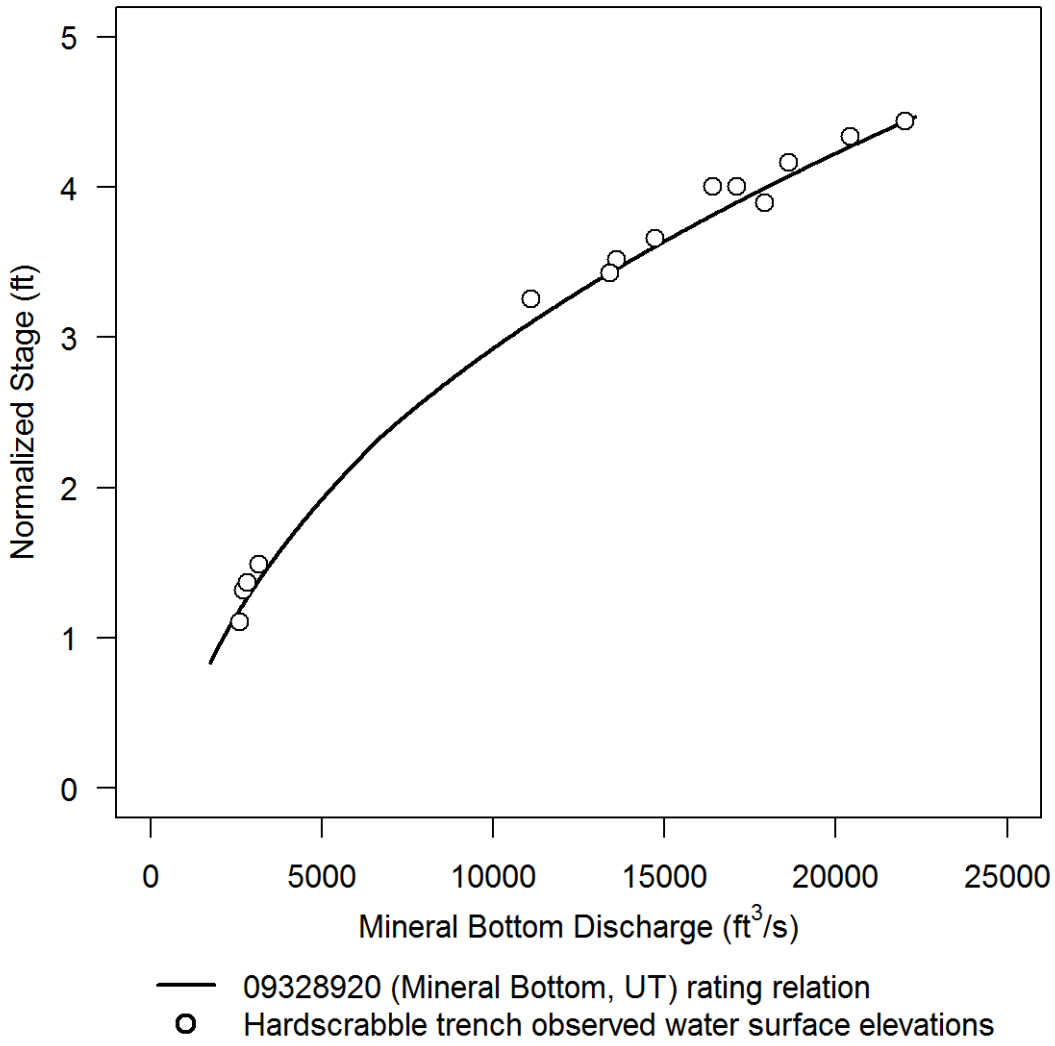

Figure 5: Stage discharge relation at Hardscrabble trench site compared to the current USGS rating relation for discharge at Mineral Bottom. Stage at both sites is normalized to an arbitrary elevation to make direct comparisons easier.

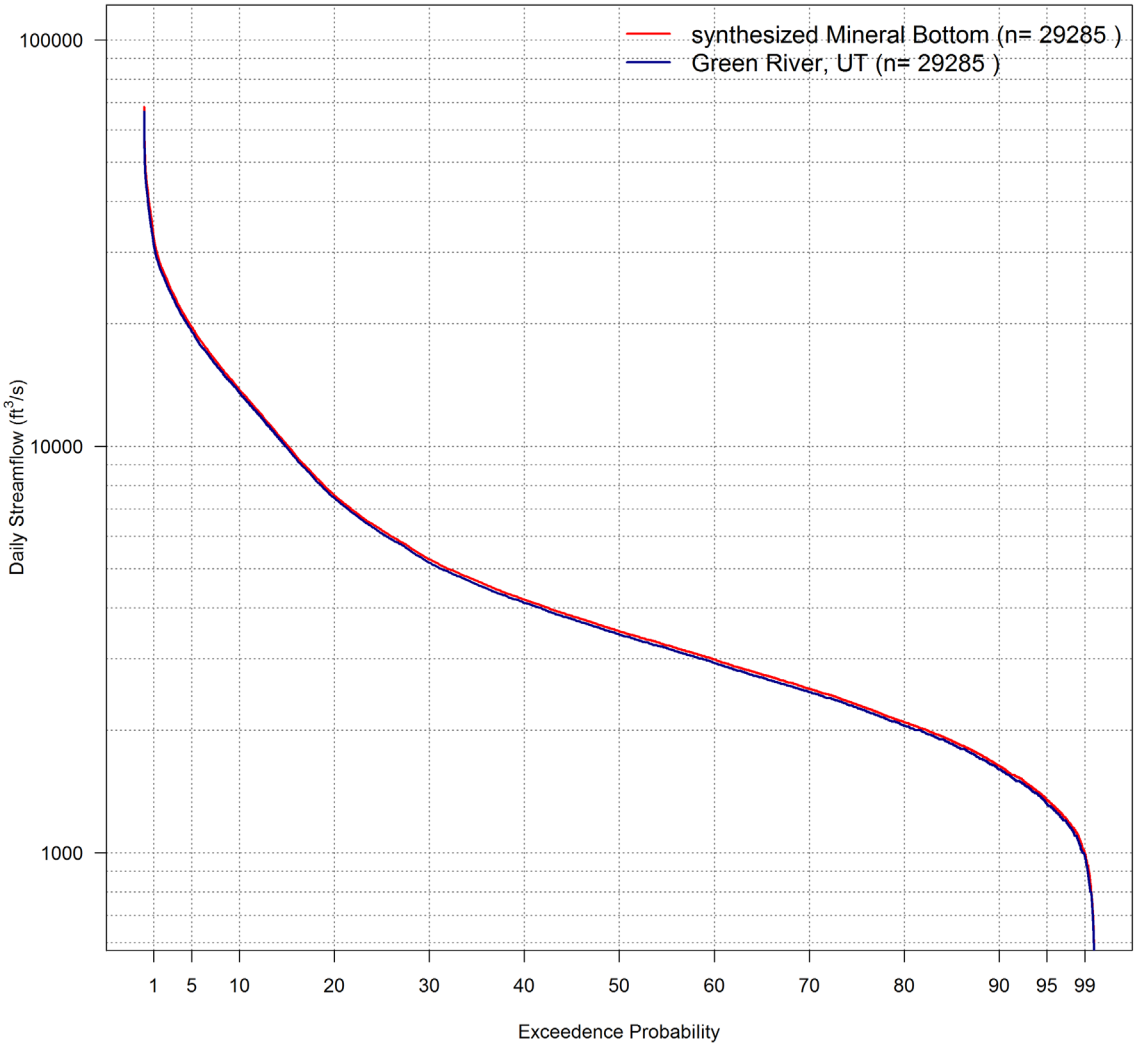

Figure 6: Flow duration curves for Mineral Bottom and Green River, UT, comparing the estimated and observed record from 1909-1918 and 1945-2015.

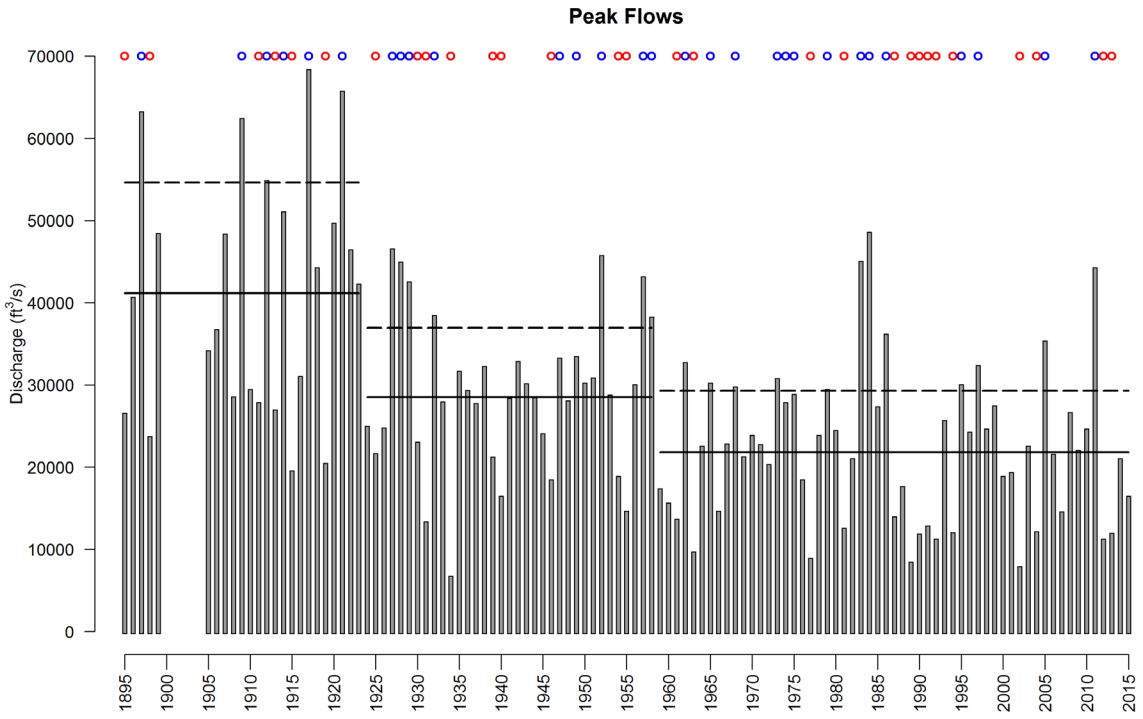

Figure 7: Time series of instantaneous annual peak flows at Green River, Utah . The 2-year (solid line) and 5-year (dashed line) recurrence intervals are shown for each period of flow regime determined by the Pettitt test. High (blue circles) and low (red circles) peak flow years are identified as defined in the text.

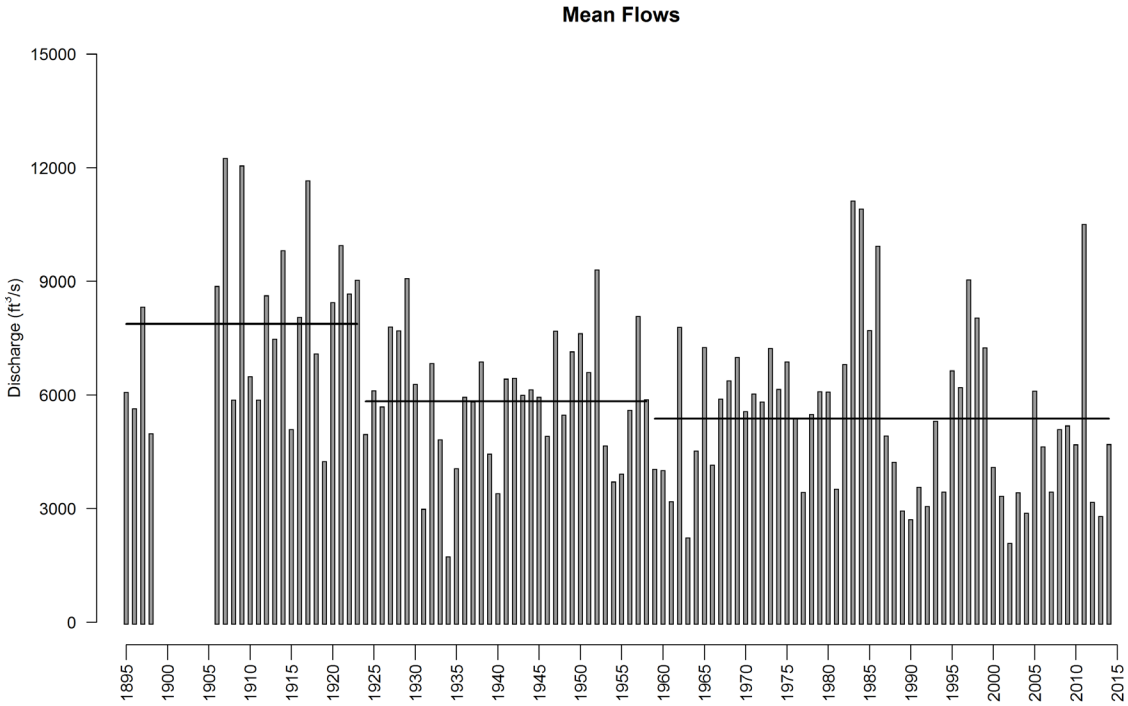

Figure 8: Mean annual flows at Green River, Utah showing mean annual flow for period of flow regime identified by a Pettitt test of instantaneous annual peak flows.

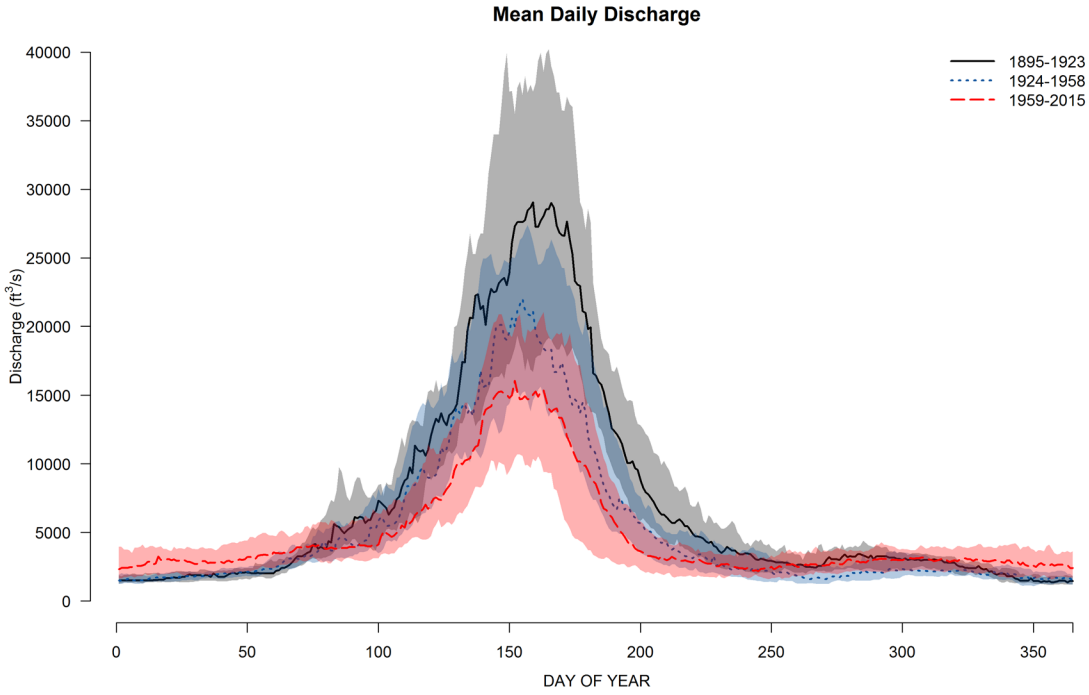

Figure 9: Mean daily discharge at Green River, Utah for each period of flow regime identified by a Pettitt test of instantaneous annual peak flows. Shaded areas show the interquartile range for each period of flow regime.

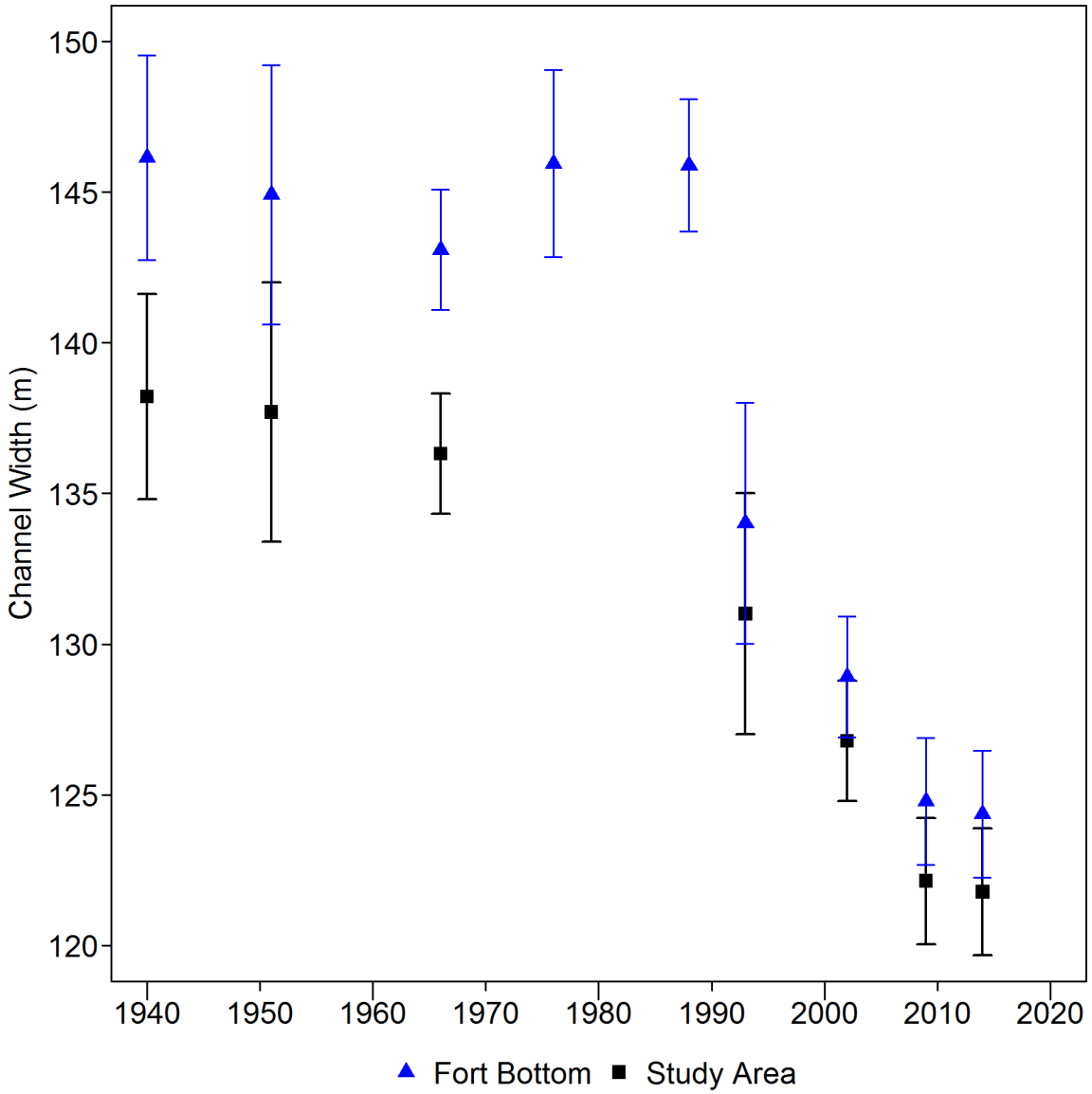

Figure 10: Changes in channel width for all years of aerial imagery segment showing A) mean channel width in the 61-km study area for each year with error bars showing spatial uncertainty (E_w). Maximum channel width decreased by 63 m from 1988 to 1993, minimum width remained stable from 1940 to 2014 and A) mean channel width in the 15-km Fort Bottom segment for each year with error bars showing E_w.

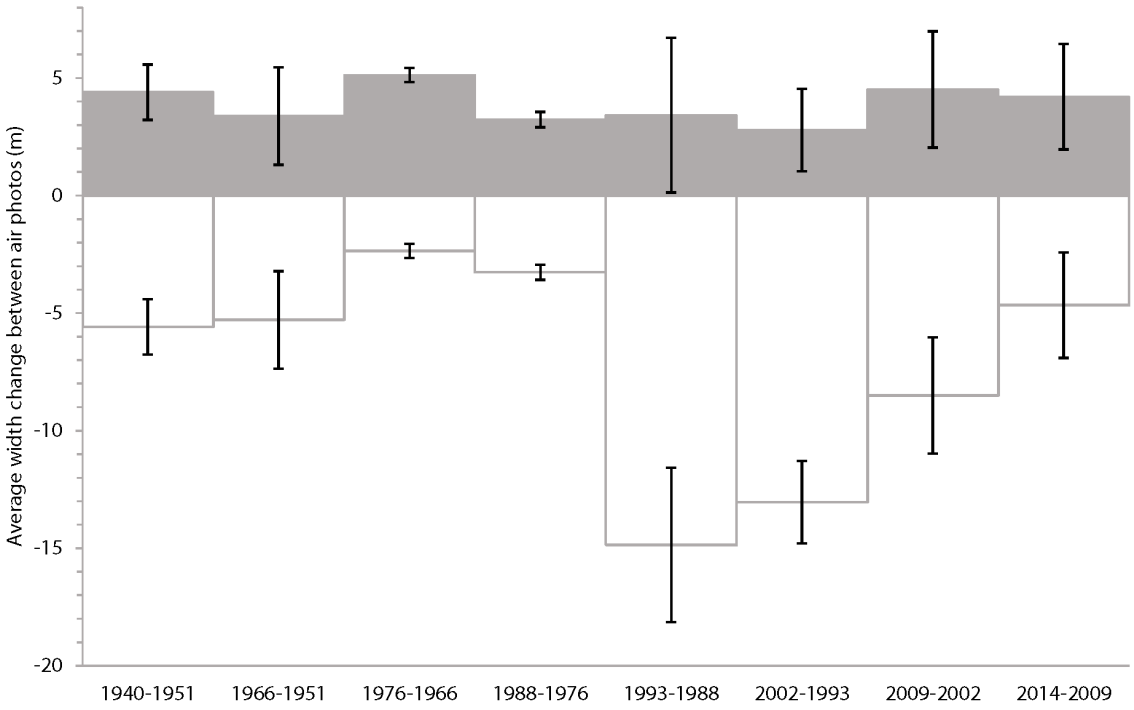

Figure 11: Net changes in active channel width by floodplain formation (white boxes) and floodplain erosion (gray boxes). Net narrowing over the Fort Bottom segment includes floodplain deposition in every single year, but that deposition is outweighed by a greater amount of erosion. Error bars represent uncertainty associated with active channel boundary digitization (*p*) in Table 3.

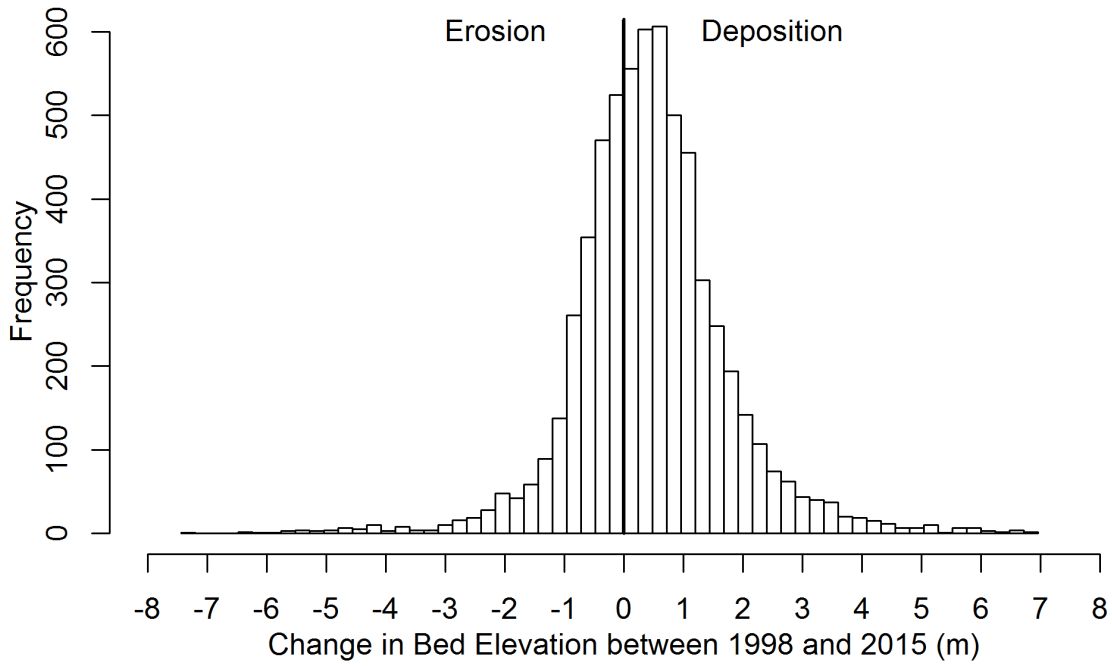

Figure 12: Histogram of differences between 1998 survey points and 2015 elevations located within the boundaries of the active channel (n = 1194).

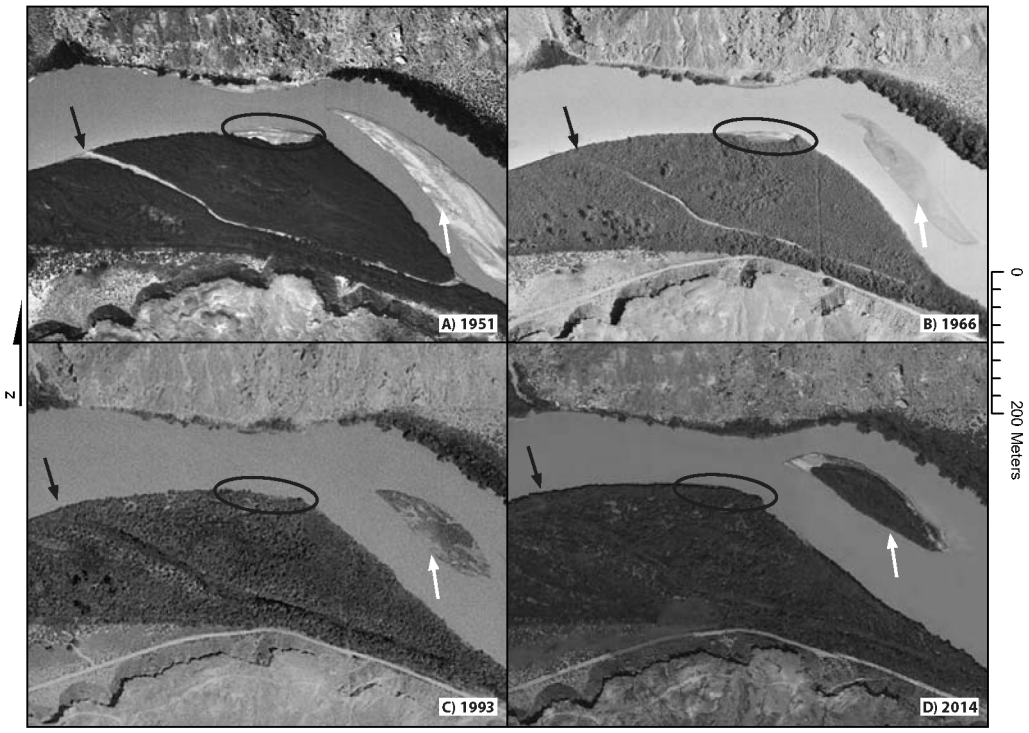

Figure 13: Channel conversions at Point Bottom, 4.8-km downstream of the Mineral Bottom gage. Flow is from right to left. A secondary channel exists in 1951 (A, Q = 2,300 ft3/s), creating a large vegetated. The open channel is clearly seen at the downstream end of the bar (black arrow). In 1966 (B, Q = unknown), vegetation has established in the upstream and downstream ends of the channel (black arrows). The secondary channel is fully vegetated in 1993 (C, Q = 13,700 ft3/s) and 2014 (D, Q = 3,820 ft3/s, black arrows). Mid-channel bar conversion occurs immediately offshore of Point Bottom (white arrows), converting an emergent bar in 1966 to a partially vegetated island in 1993 and a fully vegetated, stable island in 2014. Floodplain formation is shown within the black circles, where a bare sand bar in 1951 shrinks in area due to vegetation in establishment in 1966 and fully converts to vegetated floodplain in 1993. Floodplain and bar conversion were the primary methods of floodplain formation in the lower Green River. The mid-channel bar, before and after conversion to island, has a stable location and does not migrate downstream.

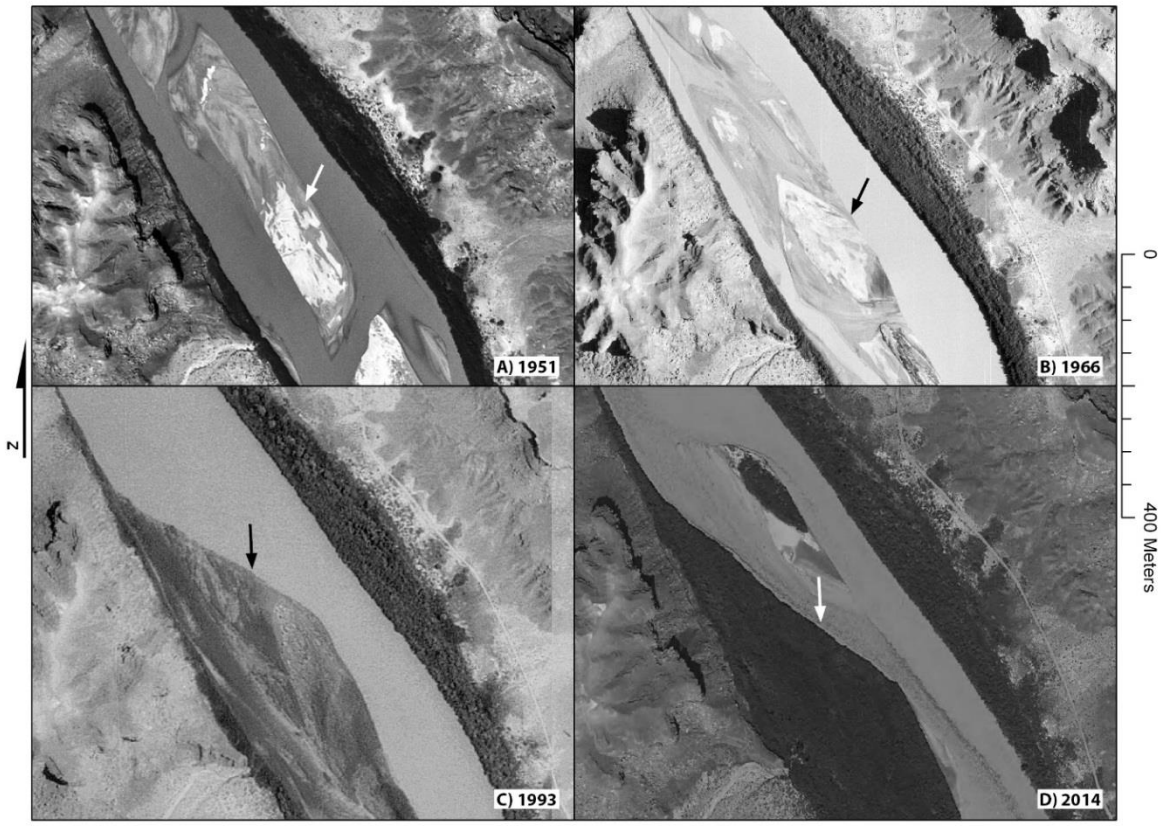

Figure 14: Conversion of a bare sand bar to vegetated floodplain at Potato Bottom (RM 36.5), within the Fort Bottom segment. Flow is from top to bottom. An active mid-channel bar in 1951 (A, Q = 2,300 ft^3/s) is located in the middle of the channel. The white arrow in A) shows the mid-channel bars. In 1966 (B, Q = unknown), the black arrow points to a mid-channel bar on river right. In 1993 (C, Q = 13,700 ft^3/s), the bar is now a bank-attached bar and vegetation has established (black arrow). By 2014, the bar (white arrow) is heavily vegetated and is part of the floodplain (D, Q = 3,820 ft^3/s).

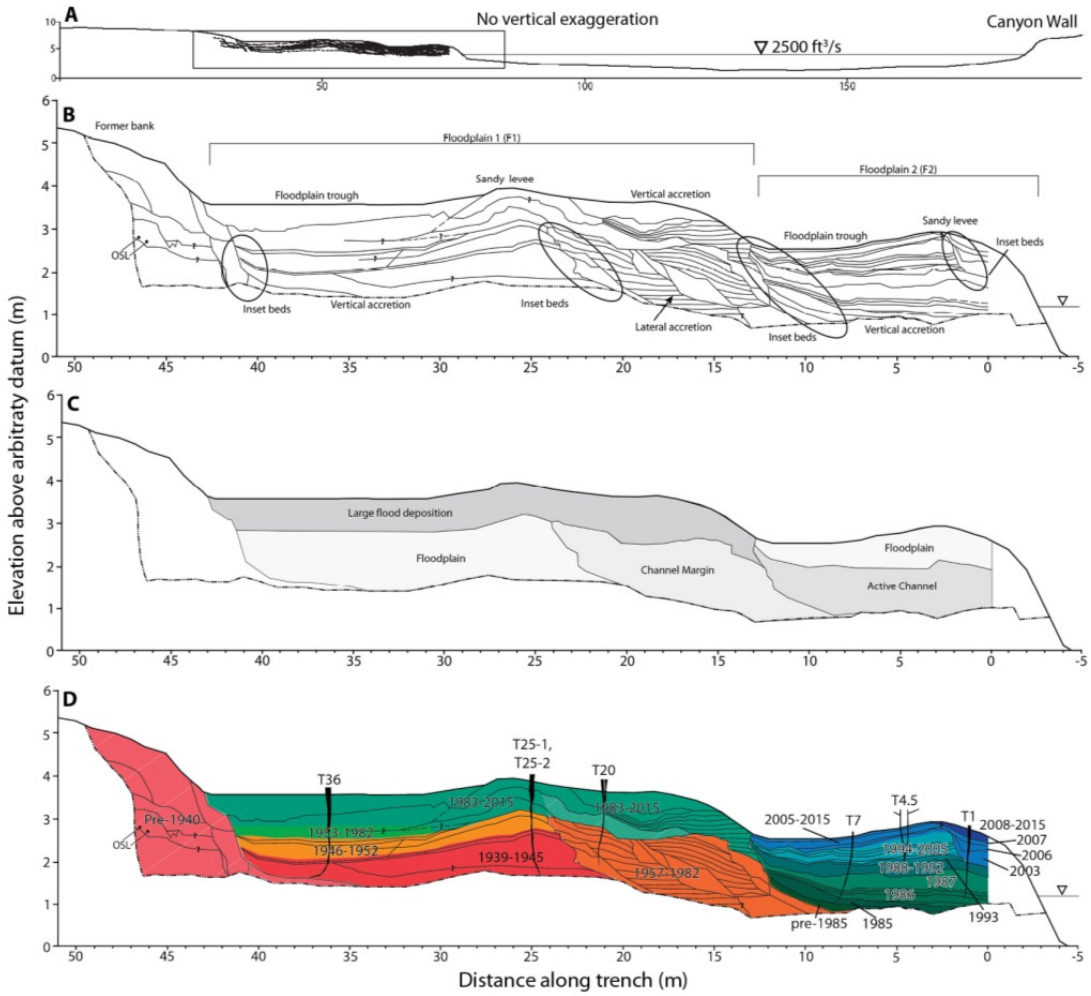

Figure 15: Trench stratigraphy and dendrogeomophology. A) Complete cross section profile shown with no vertical exaggeration. The box in A covers the trench and is the location of B, C and D. B) Stratigraphy and major features of the trench. The major inset beds are shown by the black circles. C) Major depositional facies identified in the trench. D) Locations of tamarisk trees removed from the trench and the timing of deposition resulting from tree-ring dating and OSL sampling.

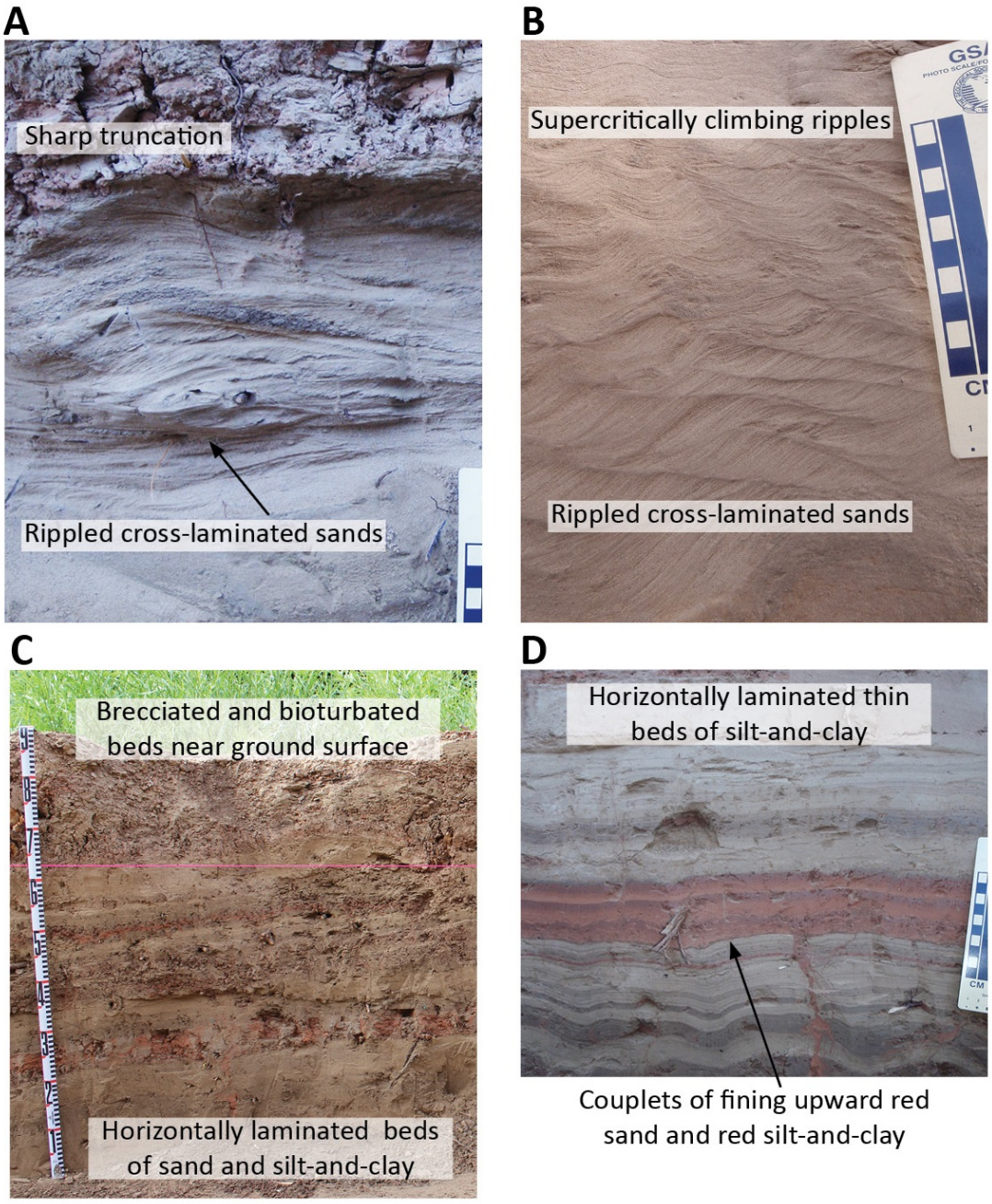

Figure 16: Typical sedimentological characteristics observed in floodplain facies. A) Rippled cross-laminated sand migrating onshore, truncated sharply at top by mud. Mud-dominated beds occur periodically in the F2 levee, but are not dominant. B) Sand beds in the F1 levee. In addition to rippled cross-laminated sand migrating onshore, supercritically climbing ripples were present, showing evidence of rapid deposition. In C), the F2 trough, horizontally laminated beds of sand and mud are present, with distinctive beds of red mud. The F1 trough, D), is dominated by mud and contains few beds of sand. Presumably, red sands and muds are locally sourced.

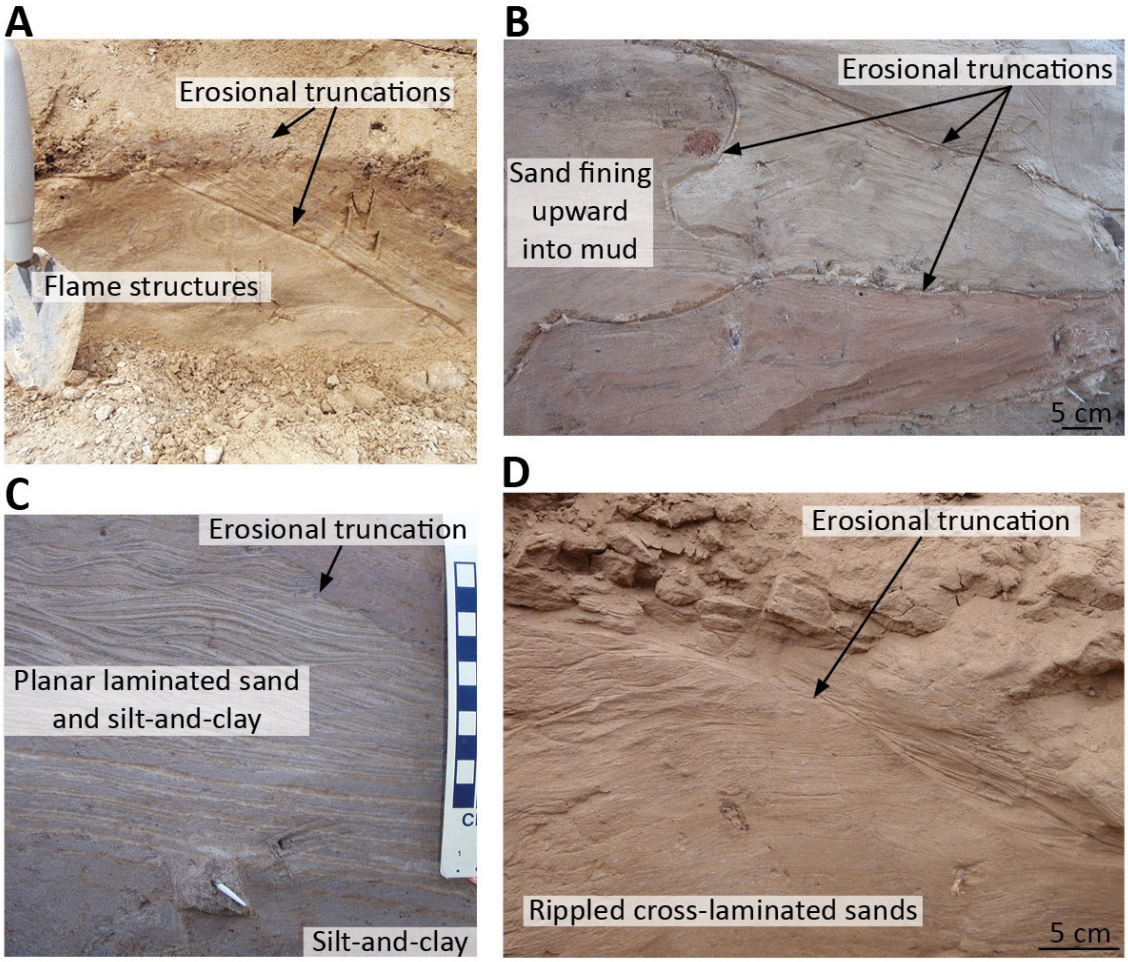

Figure 17: Sedimentological characteristics of the channel margin facies. A) Sharp, unconformable truncations which we interpreted as erosional boundaries and flame structures, indicative of rapid deposition and soft sediment deformation. B) Repeated erosional truncations and sand fining upward into mud. C) Mud converting to laminated sand and mud, then transitioning to cross-laminated sand and muds, truncated at the top by mud. D) Cross-laminated sands, sharply truncated by cross-laminated sands.

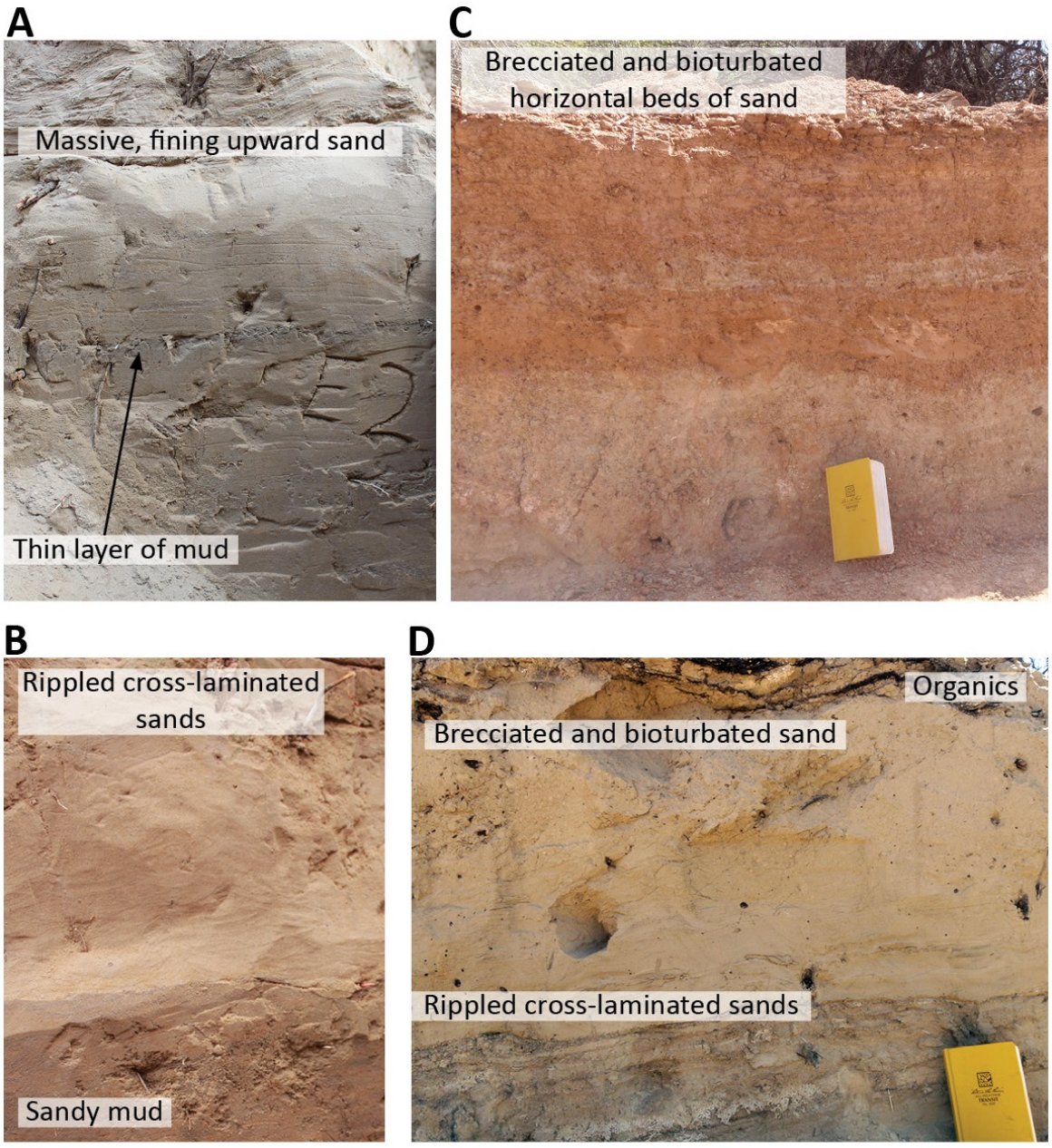

Figure 18: Sedimentological characteristics of the active channel and large flood facies. A) Massive, fining upward sand beds, divided by a thin layer of mud. Deposits in the floodplain conversion component generally have more mud than the floodplain component. Sedimentary structures are present (B), but are less frequent. In the overbank depositional component, sands and muds are brecciated and bioturbated near the surface. C) Horizontal beds of sand and red sand. D) Rippled cross-laminated sands at the base of the overbank depositional facies transition to brecciated and bioturbated sand at the top. Layers of organic soil horizons are present at the top of the facies near St. 25.

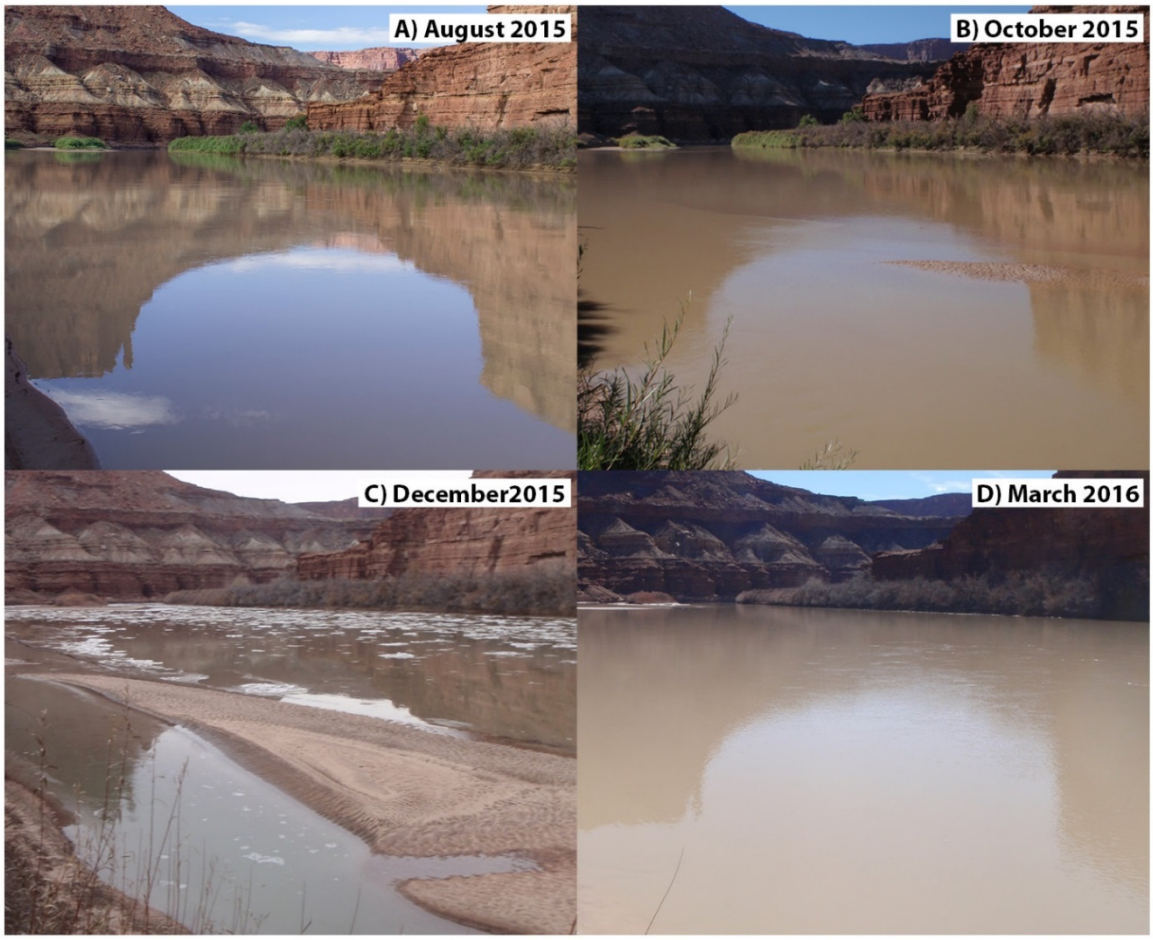

Figure 19: A photo match taken at the Hardscrabble trench, showing offshore bar deposition and erosion in summer and fall low flows. Photos are looking downstream. A) Photo taken August 7, 2015 at 2,610 ft^3/s, B) Photo taken October 15, 2015 at 2640 ft^3/s, C) Photo taken December 6, 2015 at 2,820 ft^3/s and D) Photo taken March 2016 at 3,400 ft^3/s. Discharge values are from the Mineral Bottom gage. The highest flow in this time period was 6,650 ft^3/s on October 20, 2015.

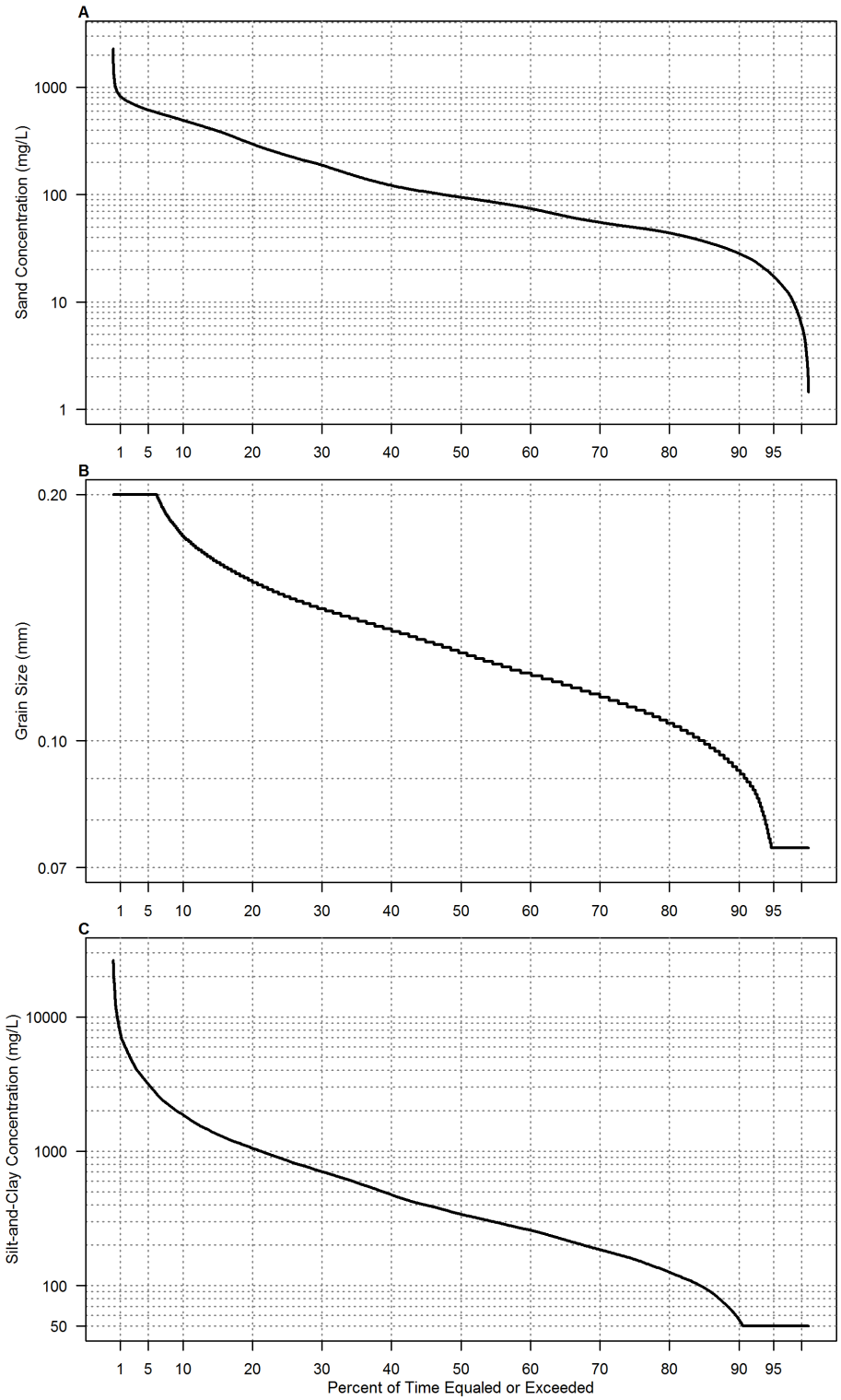

Figure 20: Duration curves for A) suspended sand concentration, B) suspended sand median grain size and C) suspended silt-and-clay concentration collected by acoustic sediment monitoring at Mineral Bottom. Concentrations of suspended silt-and-clay are almost an order of magnitude greater than concentrations of suspended sand.

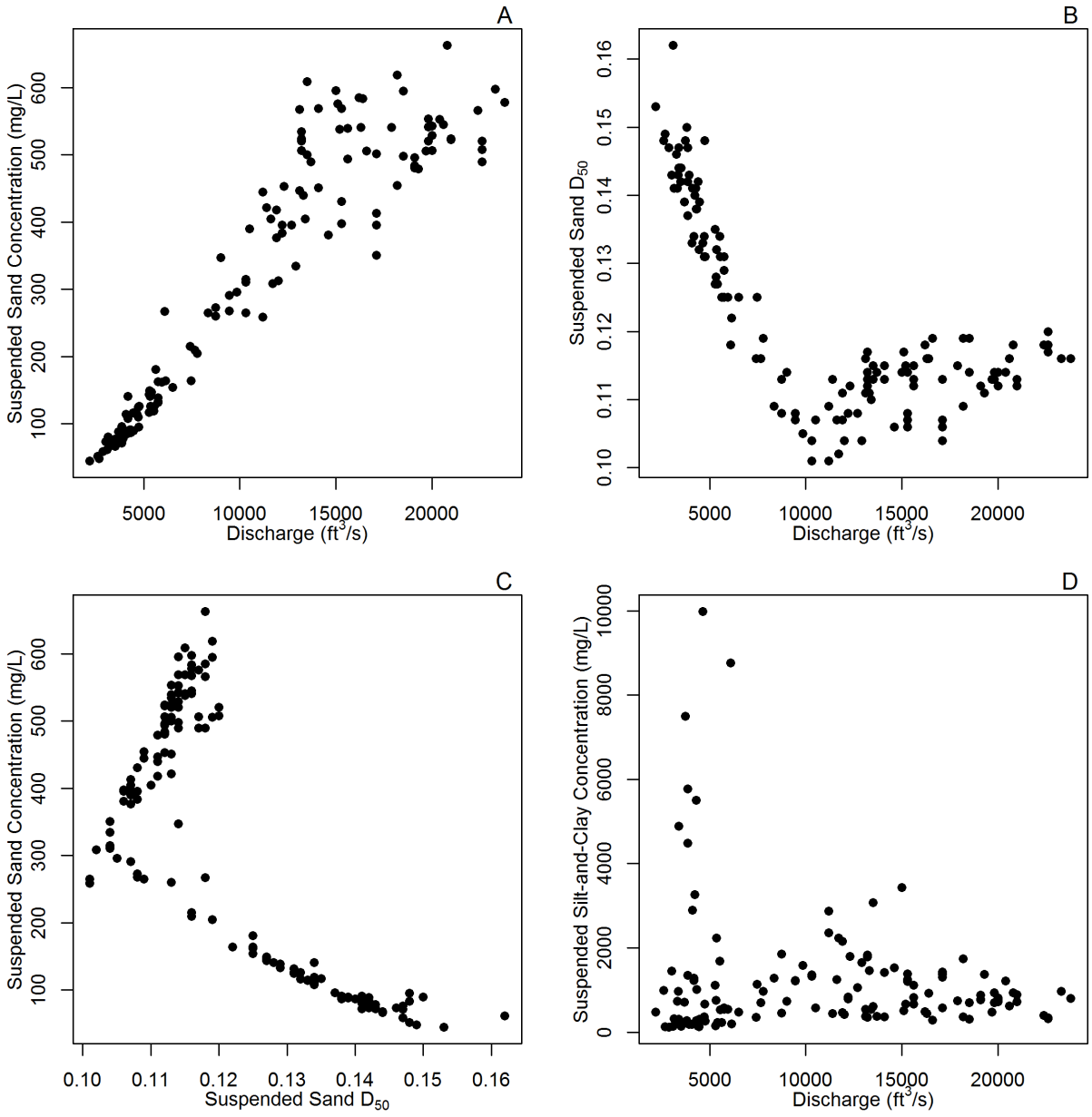

Figure 21: Characteristics of physical suspended sediment samples collected by ISCO pump sampler at Mineral Bottom from March 2014-October 2016 (n=133). A) Suspended sand concentrations increase with rising discharge. B) Median suspended sand grains size decreases with increasing discharge until 10,000 ft³/s, then increases slightly. C) Suspended sand decreases in relation to increasing median grain size. D) Suspended silt-and-clay remains relatively constant with increasing discharge.

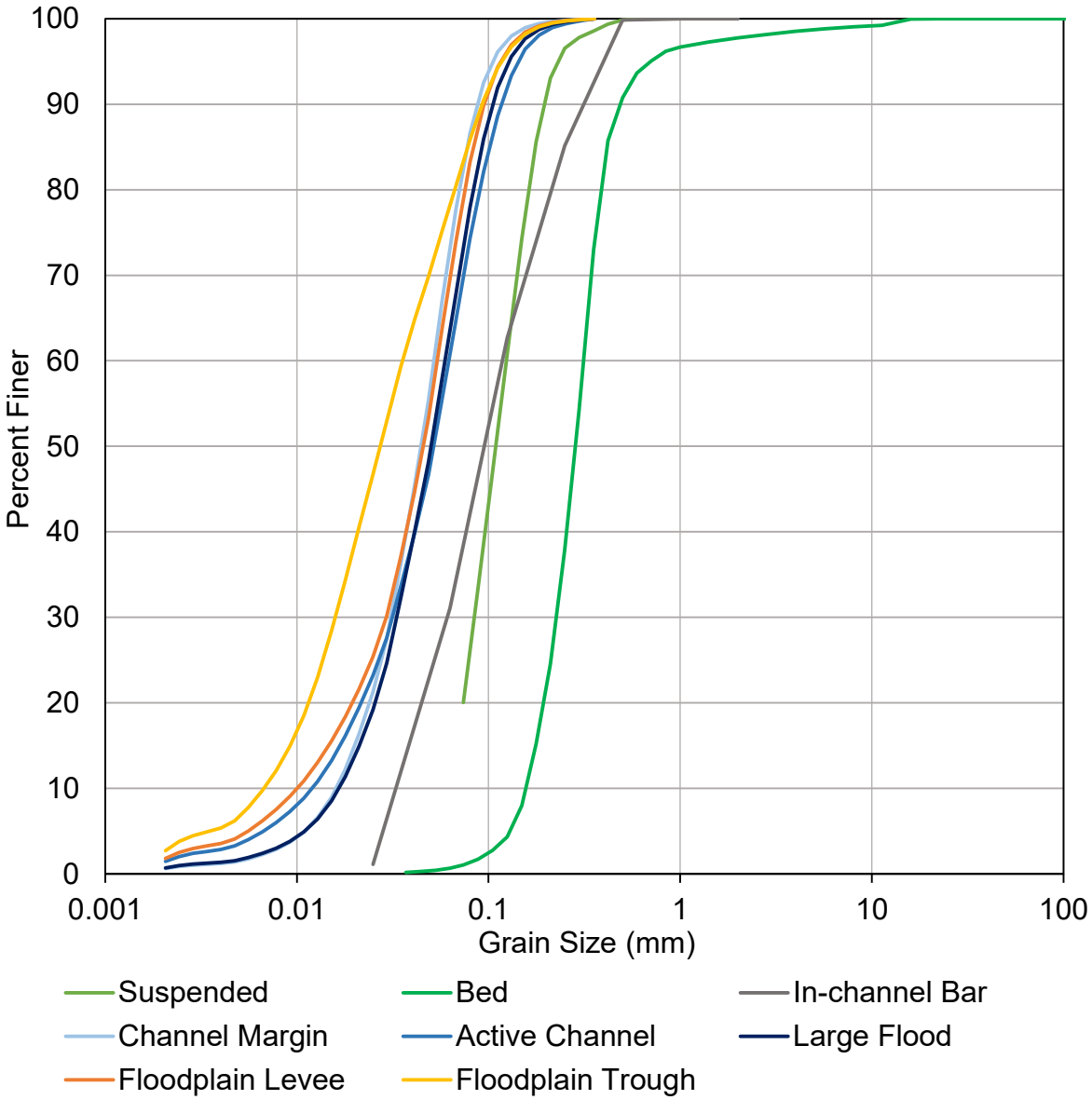

Figure 22: Grain-size distribution of sediments collected in the lower Green River. The suspended and bed sediments (in shades of green) are from physical samples collected from cross-sections at Mineral Bottom to calibrate acoustic suspended sediment monitoring. In-channel bar sediments, in gray, were collected from exposed in-channel bars near Fort Bottom and the trench. The remaining samples were collected from the trench and represent each facies. The floodplain facies is split into trough and levee to illustrate differences between the two parts of the facies.

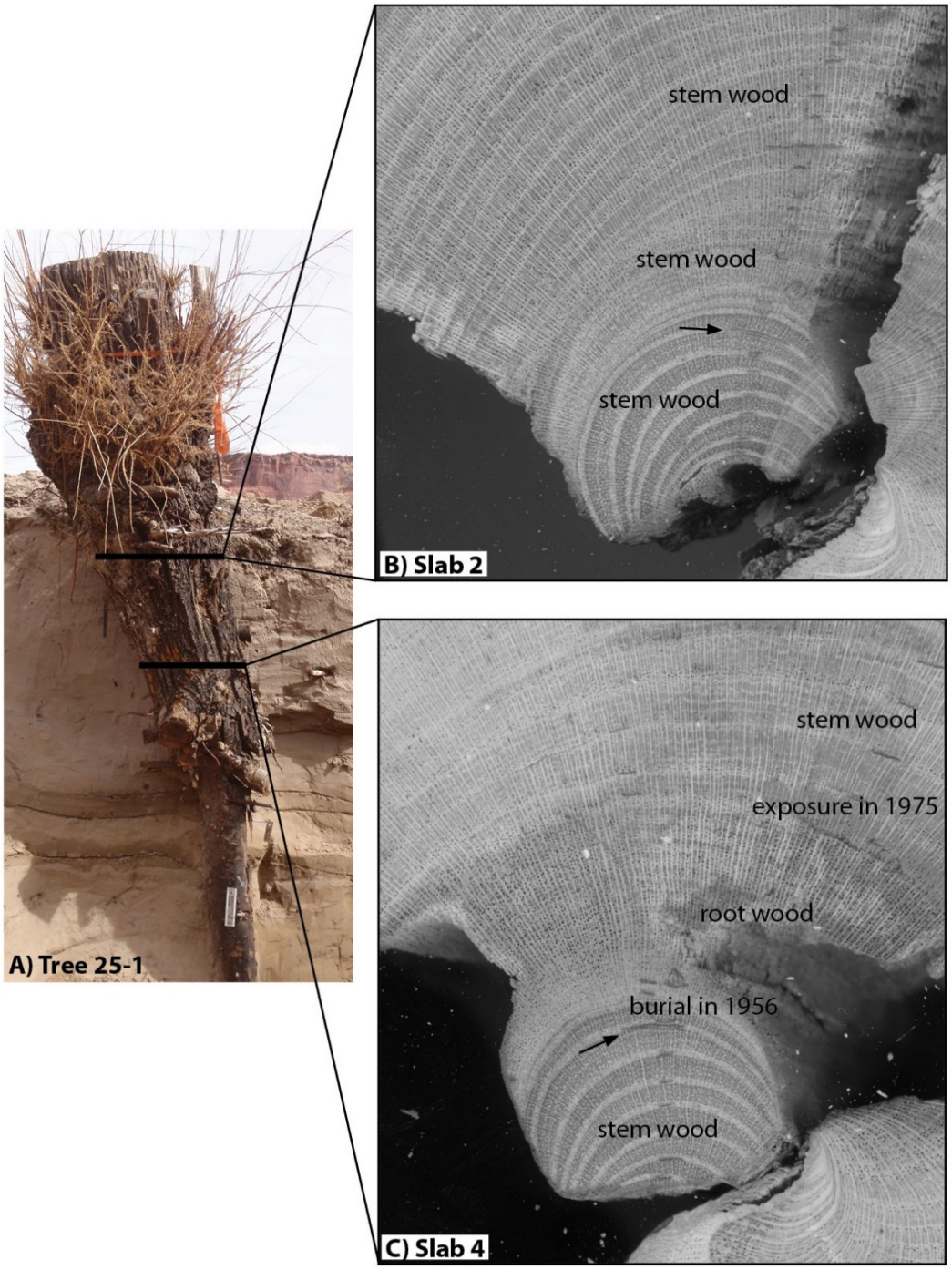

Figure 23: Burial and re-burial described in T25-1. The arrows in B) and C) point to the same growth year in both slabs. Slab 2 (B), near the surface, was never buried and its center is entirely stem wood. Slab 4 (C), at a lower elevation was initially buried in 1956, converting stem wood to root wood. The stem of the tree was re-exposed (likely due to floodplain erosion) in 1975 and the anatomy of the tree responded, adding stem wood. The tree was buried again in 1983.

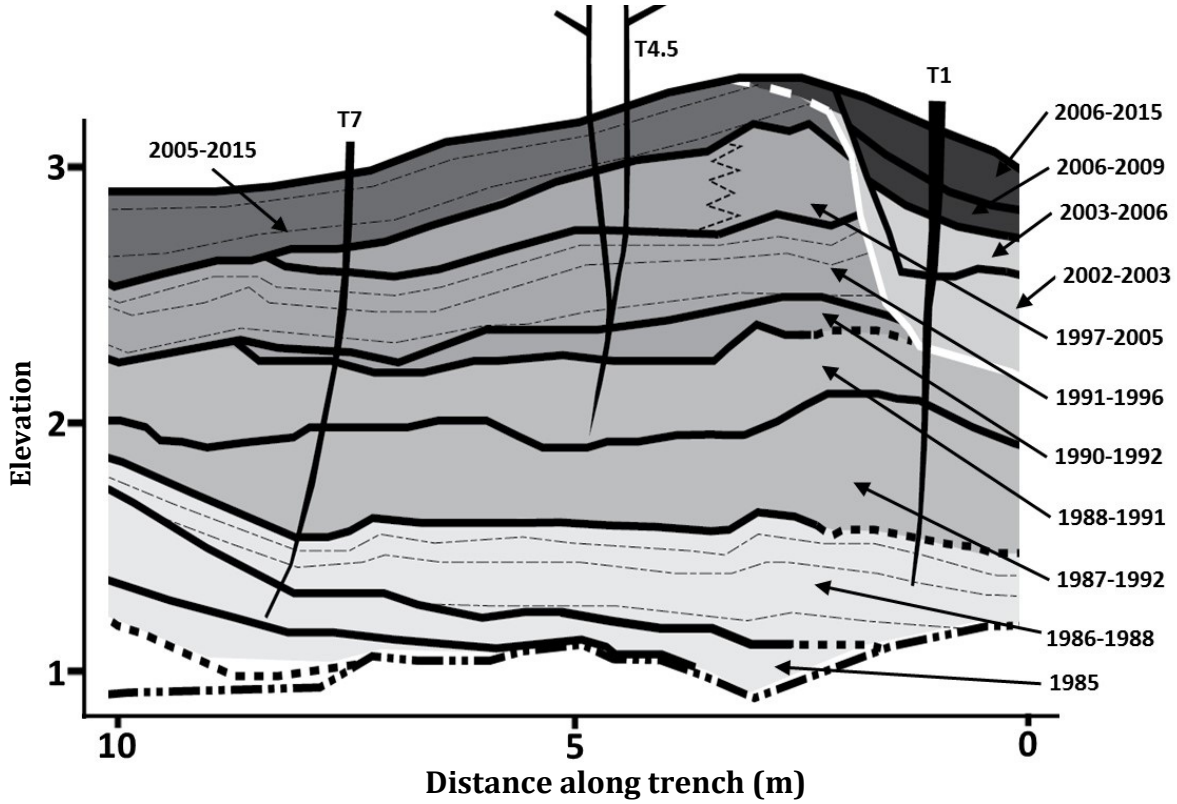

Figure 24: Close up of F2 part of trench showing uncertainty in tree-ring dating of sediments. The ages of beds in F2 overlap due to the differing burial dates for T4.5 in the levee and T7 in the trough. All deposition in F2 occurred in 1985 or later. The uncertainty shown here was constrained with the stage discharge relation in Figure 3.3 to produce the ages of deposition discussed in text and shown in Figure 15D.

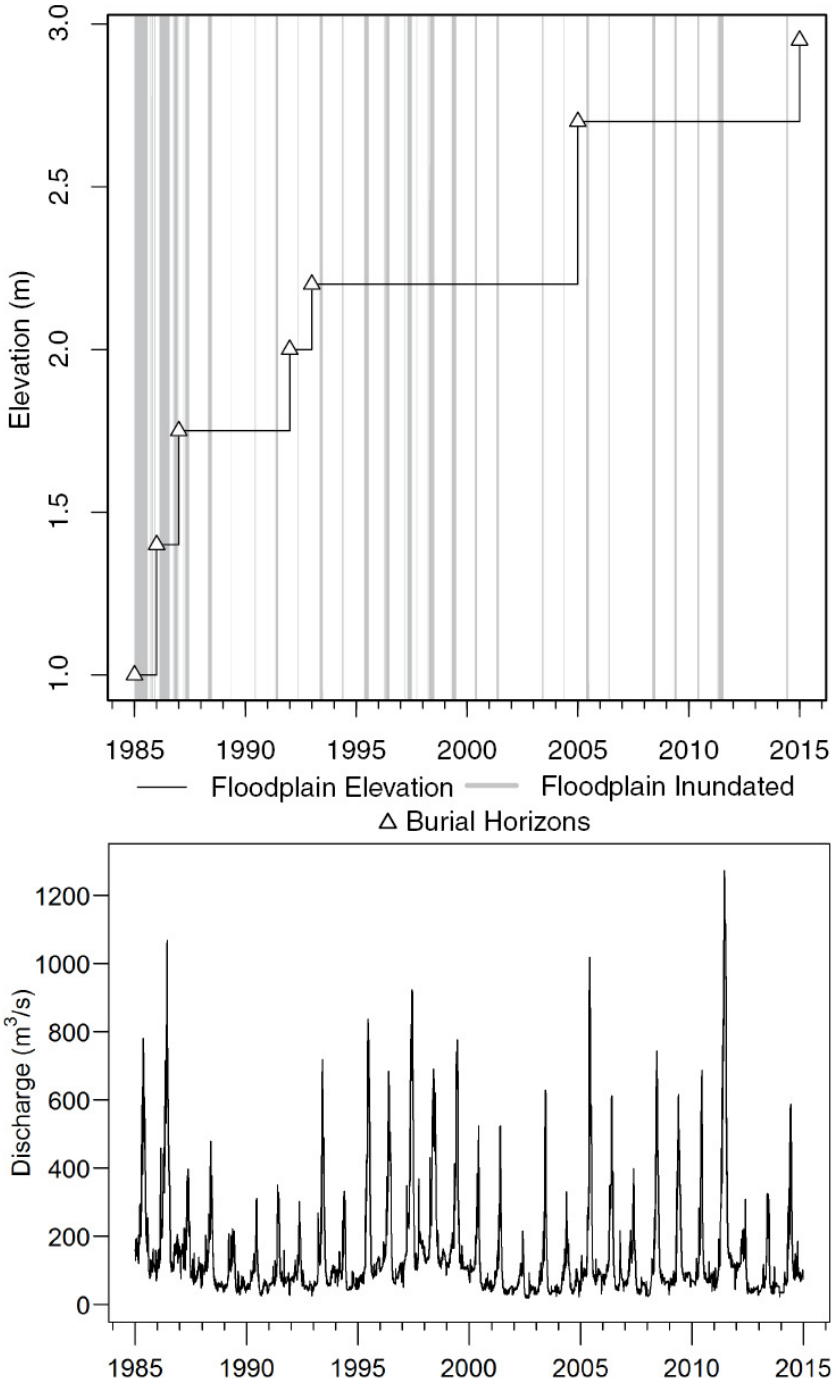

Figure 25: Plot of floodplain elevation for post 1985-deposits and daily discharge for same time period (1985-2015). On the upper plot, the elevation of the floodplain is represented by the black line and time when the floodplain was inundated by blue shaded areas. Triangles represent ages of stratigraphic contacts determined by dendrogemorphology aging. For the inset floodplain which formed after 1985, the amount of time it was inundated decreased substantially after 1987, but was still inundated on a 1.5-2 year recurrence interval until 2011. Adapted from Allred and Schmidt (1999).

Table 1: Flow regime periods identified from Pettitt test

Period	Number of Years	Mean Annual Flow (ft^3/s)	2-year flood (ft^3/s)	5-year flood (ft^3/s)	P-value of break point*	25th percentile flow (ft^3/s)	75th percentile flow (ft^3/s)
1985-1923	23	7,870	41,200	54,600		28,100	49,800
1924-1958	34	5,830	28,500	36,900	0.015	23,300	32,800
1959-2016	58	5,370	21,800	29,300	3.87x10-6	14,300	27,200

*Two break points exist, 1 in 1924 and 1 in 1959

Table 2: Aerial imagery information

Year	Dates	Agency	Film Type	Approximate Scale	Pixel resolution (m)	Discharge (ft^3/s)	Coverage of study area (%)
1940	8/30	US Department of Agriculture (USDA)	Black & White	31,680	1	3,950	90
1951	9/19	US Geological Survey (USGS)	Black & White	20,000	0.5	2,300	79
1966	Unknown	Bureau of Land Management	Black & White	15,840	1	Unknown	100
1976	8/31	National Park Service (NPS)	Color	12,000	0.15	3,040	28
1988	8/27	Bureau of Reclamation	Color Infrared	6,000	0.15	1,820	25
1993	6/14	USGS	Black & White	40,000	1	13,700	100
2002	6/18 and	USGS/NPS	Color	12,000	0.84	2,370	99
2009	8/7	USDA Aerial Photography Field Office (APFO)	Digital Color	-	1	3,100	100
2011	6/22	USDA APFO	Digital Color	-	1	42,300	100
2014	9/11	USDA APFO	Digital Color	-	1	3,820	100

Table 3. Errors associated with aerial imagery analysis and channel measurements derived from image analysis. All values are in meters.

Year	Channel widths						Width error analysis		
	All			Fort Bottom					
	Mean	Min width	Max width	Mean	Min width	Max width	Feature identification error (p)	Image distortion error (θ)	Total width error (E_w)
1940	138	89	237	146	97	237	1.9	2.9	3.4
1951	138	91	239	146	100	234	1.7	4.0	4.3
1966	136	90	251	143	94	227	1.5	1.4	2.0
1976	N.A.*	N.A.	N.A.	146	97	234	1.4	2.7	3.1
1988	N.A.	N.A.	N.A.	146	92	231	1.5	1.6	2.2
1993	131	87	189	134	87	167	2.3	3.2	4.0
2002	127	85	183	129	85	167	1.5	1.4	2.0
2009	122	87	171	125	87	158	1.7	1.2	2.1
2014	122	83	169	124	85	154	1.6	1.4	2.1

*N.A. – Not applicable

Table 4. Hell Roaring Canyon repeat cross-section measurements

Date	Discharge (ft^3/s)	Mean Depth (m)			Maximum Depth (m)			Width (m)			Width/Mean Depth Ratio		
		MB2	MB3	MB4	MB2	MB3	MB4	MB2	MB3	MB4	MB2	MB3	MB4
6/24/1995	26,000	4.4	4.5	4.9	7.7	9.5	8.4	133.2	135.5	144.3	30.6	30.2	29.2
7/20/1995	12,600	4.6	4.8	5.4	6.9	7.6	9.7	135.6	136.7	146.3	29.2	28.4	26.9
8/11/1995	3280	5.1	5.1	5.9	7.1	7.1	10.3	135.4	135.4	146.3	26.6	26.3	24.6
5/28/1996	17,700	4.9	5.5	5.2	6.6	7.8	9.3	135.7	136.8	146.4	27.9	24.8	28.2
7/1/1996	10,300	4.9	4.8	5.0	7.0	7.1	8.1	135.7	136.9	146.7	28.0	28.3	29.5
8/27/1996	2150	5.1	5.0	5.2	6.9	7.4	8.7	135.9	136.8	146.5	26.7	27.2	28.2
10/18/1996	2680	5.3	5.0	4.7	7.0	7.0	7.5	135.8	136.8	146.5	25.6	27.6	31.0
5/15/2015	10,800	6.0	6.0	6.1	8.0	8.0	8.8	135.7	136.9	146.4	22.6	22.8	24.1

Note: Cross-sections listed are for the three cross sections where a measurement was collected on every date. Cross sections are located 5-km upstream of the Mineral Bottom gage, at the mouth of Hell Roaring Canyon

Table 5: Optically Stimulated Luminescence Age Information.

Sample	Depth below ground surface (m)	Grain Size (mm)	Number of grains*	Dose Rate (Gy/ka)	D_E †± 2σ (Gy)	OD^ (%)	OSL age ± 2σ (ka)
HRD-OSL-1	1.67	.150-.200	65 (2000)	2.32 ± 0.10	0.69 ± 0.33	71.4 ± 15.9	0.30 ± 0.15
HRD-OSL-2	1.76	.150-.200	63 (1900)	2.05 ± 0.09	0.91 ± 0.50	75.2 ± 17.8	0.44 ± 0.25

*Number of grains used in age determination, total grains measured in parentheses

†Equivalent dose calculated by the minimum age model of Galbraith and Roberts (2012)

^Overdispersion represents variance in D_E, an OD large than 20% may indicate scatter by depositional or post-depositional processes

Table 6: Clay minerals XRD information by weight percent

Sample ID	Color in Field	Quartz	K-feldspar	Plagioclase	Calcite	Dolomite	Ank. or exc-Ca Dol.	*Total Carbonate*	Pyrite	Gypsum	Hematite	Clinoptilolite /Analcime	*SUM NON-CLAY*	Kaolinite group	Chlorite	Illite+Smectite group	% S est in I-S	*SUM CLAY*	is the mineral more illitic or smectitic?
10.7C-Red	Red	23	7	2	6	4	3	*12*	0	1	1	0	***45***	5	2	48	12	***55***	illitic
10.7C-Grey	Grey	20	6	5	5	3	1	*9*	0	1	0	7	***49***	8	1	42	54	***51***	smectitic
10.7 Cup	Red	28	8	2	5	5	3	*12*	0	0	1	0	***51***	4	1	44	11	***49***	illitic
8.7 Gsub	Tan/Grey	23	6	4	10	3	2	*15*	1	0	0	3	***51***	4	1	44	48	***49***	smectitic
10.7 F	Tan/Grey	29	8	6	7	4	3	*14*	0	0	0	2	***59***	2	2	37	47	***41***	intermed IS
34.0X	Red	37	9	2	5	2	6	*12*	0	0	1	0	***61***	2	1	36	10	***39***	illitic
34.0Y	Grey	32	8	8	8	4	2	*14*	1	0	0	6	***68***	4	2	26	48	***32***	smectitic
34.0W	Grey	31	8	6	9	4	3	*16*	0	0	0	3	***65***	4	1	30	36	***35***	intermed IS
34.0Z	Red	27	7	2	5	4	2	*10*	0	0	2	0	***48***	4	2	46	9	***52***	illitic
GR1	Grey	31	6	3	8	7	1	*15*	0	0	0	2	***56***	5	2	37	42	***44***	intermed IS
UPH1	Red	77	10	1	3	0	3	*6*	0	0	0	0	***95***	0	0	4	6	***5***	illitic
UPH2	Red	81	10	1	3	0	3	*5*	0	0	0	0	***96***	0	1	3	ND	***4***	ND
UPH3	Red	75	11	1	2	2	2	*5*	0	0	0	0	***92***	0	1	7	< 5	***8***	illitic
PR1	Grey	67	3	3	16	2	1	*19*	0	0	0	1	***94***	1	1	4	43	***6***	intermed IS
PR2	Grey	75	4	4	5	3	1	*9*	0	0	0	0	***92***	1	0	7	< 5	***8***	illitic

Ank. or exc-Ca Dol. = Ankerite or excess-Ca dolomite
Illite+Smectite group = total dioctahedral 2:1 layer clay: illite, mixed-layer illite-smectite, smectite, and possibly mica.
Biotite group = total trioctahedral 2:1 layer clays: biotite, phlogopite, biotite/vermiculite, trioctahedral smectites
Serpentine group = total trioctahedral 1:1 layer clay: serpentine-type minerals and berthierine
Kaolinite group = total dioctahedral 1:1 layer clay: kaolinite, dickite, nacrite, halloysite
Siderite, Sphalerite, Halite, Barite and Anhydrite groups all recorded 0% for all samples.